Title

Development of Molecular Probes for the Detection of Infectious Viruses and Screening of Anti-Viral Agents

Permalink

https://escholarship.org/uc/item/5x1187fp

Author

Sivaraman, Divya

Publication Date

2011

Peer reviewed|Thesis/dissertation

UNIVERSITY OF CALIFORNIA

RIVERSIDE

Development of Molecular Probes for the Detection of Infectious Viruses and
Screening of Anti-Viral Agents

A Dissertation submitted in partial satisfaction
of the requirements for the degree of

Doctor of Philosophy

in

Chemical and Environmental Engineering

by

Divya Sivaraman

December 2011

Dissertation Committee:
        Dr. Wilfred Chen, Co-Chairperson
        Dr. Nosang Myung, Co-Chairperson
        Dr. Ashok Mulchandani
        Dr. Marylynn V. Yates

The Dissertation of Divya Sivaraman is approved:

_____

_____

_____

Committee Co-Chairperson

_____

Committee Co-Chairperson

University of California, Riverside

Acknowledgements

I would like to express my gratitude to Dr. Wilfred Chen, Dr. Marylynn V. Yates, Dr. Ashok Mulchandani and Dr. Nosang Myung for their valuable advice, support and guidance for developing this dissertation. I am also thankful to the publishers of the journal for their permission to reprint this paper.

ABSTRACT OF THE DISSERTATION

Development of Molecular Probes for the Detection of Infectious Viruses and
Screening of Anti-Viral Agents

by

Divya Sivaraman

Doctor of Philosophy
Graduate Program in Chemical and Environmental Engineering
University of California, Riverside, December 2011
Dr. Wilfred Chen, Co-Chairperson
Dr. Nosang Myung, Co-Chairperson

Viruses pose a serious threat to public health and safety. Rapid and efficient

detection of viruses is crucial for the prevention of disease spread and timely clinical

management. Traditional methods for detection of viral infection that rely on viral

isolation and culture techniques continue to be the golden standards used for detection

of infectious viral particles. However, improved methods for rapid and reliable

detection and quantification of viruses are required for public health assessment. New

techniques relying on visualization of live cells can shed some light on understanding

virus-host interaction for early stage detection and potential drug discovery. One such

technology is the use of Molecular beacons (MBs), which produce fluorescence upon

target binding and offer a simple, separation free scheme for sensitive detection of

infectious viruses. In this study, we developed several FRET (fluorescence resonance energy transfer)-based MBs combined with fluorescence microscopy to directly visualize the fluorescent hybrids with viral RNA as an indication of viral infection. To prevent nucleolytic degradation, MBs were designed containing 2'-O-methyl RNA bases with phosphorothiote linkages and a cell-penetrating Tat peptide was attached to facilitate non-invasive intracellular delivery. To demonstrate the flexibility of this technique to be adapted into a high-throughput screening method, a flow cytometry (FC) based system was utilized and the simplicity of using a flow based scheme for rapid identification of virus infected cells was demonstrated. Confluent cell monolayers were infected with virus dilutions followed by incubation with MB probes and fluorescent intensity was monitored using fluorescence microscope as well as flow cytometry. The sensitivity of the assay to detect less than 1% infected cells in a mixed cell population was shown. The illumination of fluorescent cells increased in a dose-responsive manner and enabled direct quantification of infectious viral doses. Fluorescent signal from virus infected cells was discernible as early as 15 min thereby enabling rapid detection. The specificity of the MBs to differentiate between different subtypes of viruses was also demonstrated. The specific nature of these probes enable their utility for rapid diagnosis of viral infection and provides an better understanding

of the multiple steps involved in the viral infection process, which will be valuable for the prevention and control of disease.

Another approach to detect the presence of infectious viruses was explored by probing the viral protease activity *in vivo*. Proteases are involved in many essential cellular processes and are used as the key virulence factors for pathogenic infection. These properties make proteases a prime target for detailed investigation to better understand the disease development process and to identify targets for drug treatment. The approach was to generate a quantum dot (QD)-modified, protease-specific protein module that can be utilized as a FRET based nano-biosensor for probing viral protease activity *in vivo*. The site-specific incorporation of an acceptor fluorophore was accomplished using a cysteine residue and conjugation of QDs was facilitated by the presence of a hexa-histidine tag. Simple purification of the QD-FRET substrate was achieved by the presence of an elastin like protein (ELP) and intracellular delivery of the substrates was enabled by the use of a flanking Tat peptide. The effectiveness of the FRET substrate to probe intracellular viral protease activity was studied by measuring the whole-cell fluorescence ratio between the QD and the acceptor fluorophore. The utility of the assay system was validated for high-throughput screening of viral protease inhibitors.

Table of Contents

Table of Figures

Chapter 1

Introduction

Introduction

Viruses constitute a major class of pathogens accounting for a variety of ailments ranging from common cold, which leads to loss of productivity, to acute infections, such as influenza, which can be responsible for high mortality epidemics and, in certain cases, pandemics (1, 2). Over the years a need for rapid and specific viral detection has been realized. The major reasons for this drive has been the time consuming and expensive nature of traditional viral diagnostic techniques of culture and the availability of several antiviral therapeutics. In the past decade, the rapidly evolving nature of some virus families has necessitated the use of adaptable diagnostic tools to identify the presence of newly emerging strains for treatment, because most anti-viral drugs must be administered within 48 hrs of the onset of symptoms to be most effective (3).

Until the 1980s, viral detection was solely based on traditional viral isolation and culture techniques – plaque assay, haemagglutination assay and histological observations, which even today remain gold standards in many diagnostic laboratories (4). However, these techniques are time-consuming, labor-intensive, and culture-based methods that are not suitable for viral classes that are difficult to cultivate in the laboratory environment. Several direct examination techniques, such as immunofluorescence, enzyme linked immunosorbent assay (ELISA) and electron microscopy, have also been used for viral particle detection, although they suffer from poor sensitivity and specificity, making it difficult to interpret the results (5). In the 1990s, highly sensitive molecular methods based on amplification of nucleic acids using PCR took center stage, and quantitative

PCR (qPCR), which employs fluorescent probes, has shown greater success owing to the ease of standardization and higher sensitivity (6). However, most of these above mentioned techniques serve primarily as detection tools and provide minimal information on infectivity. In addition, very few insights about the molecular mechanisms involved in viral replication and the pathogenetic events occurring within the cells can be provided by these methods. A detailed understanding of the molecular mechanisms involved in virus replication might not only lead to new and rapid detection methodologies, but will also help the design of targeted approaches to develop more powerful anti-viral compounds.

Over the last several years, researchers have begun to realize several techniques for visualizing the viral life cycle inside living cells. The focus for these studies involve: viral entry mechanisms (7); the transport of viral core molecules through the cell to the nuclear region (8); the transport of viral nucleic acids in and out of the nucleus (9); the assembly and transport of newly-synthesized viral components (10); and the cell-to-cell spread of newly-synthesized viral particles (11). These methods are mostly based on either the use of nucleic acid probes, protease activity probing, or viral coat/genetic core labeling (12-14). Detection of a wide range of viruses, such as HIV, poliovirus (PV) and influenza viruses has been achieved, even offering single molecule sensitivity (15-18).

Nucleic acid-based methods for visualizing viral infection

An in-depth understanding of mRNA expression, interaction, movement and localization provides information on cellular responses to different conditions. Live-cell imaging of mRNA provides the opportunity to study the dynamics of mRNA expression and localization, and can be an important tool for advancing disease pathophysiology, drug discovery, and medical diagnostics. In the field of virology, live-cell RNA imaging enables a detailed understanding of viral infection and pathogenesis (19). The vast majority of viruses contain RNA genomes that play a crucial role by serving as templates for the transcription of viral RNAs, which then replicate, are later translated into a protein, and finally assembled into new viral particles (20). The lack of a suitable technology has been the key limitation in the past; however, live-cell RNA imaging has recently been realized using direct fluorescent labeling (21), the use of fluorescent probes (22), and sequence-specific mRNA recognition by GFP fusion proteins (23).

Fluorescently labeled RNA

A detailed understanding of viral entry into the host cell is not only essential for developing therapies to combat viral infection, but it also provides insights into fundamental viral infection processes (7). The entry pathway of PV was recently characterized by live-cell imaging using dual-labeled virus particles (15). This was accomplished by incorporating a membrane-permeable, nontoxic Syto82 dye into the newly synthesized viral RNA before packaging, followed by labeling of the viral capsid with an amine-reactive Cy5 dye. By combining biochemical inhibition assays with direct

visualization of PV in the early infection cycle, the authors confirmed that the release of viral RNA was energy-, actin- and kinase-dependent. Similar imaging techniques are largely applicable to most non-enveloped viruses where the cellular sites of genome release are still unknown and the information obtained is valuable for designing inhibitors suitable for blocking viral entry (15).

As an improvement to the dual-labeling method, multiply labeled tetravalent RNA imaging probes (MTRIPs) have been developed to provide an accurate imaging of native mRNAs (18), particularly when delivered into live cells using streptolysin-O (SLO). An increase in the signal is achieved owing to binding of multiple probes to a single target RNA. The feasibility of tracking viral infection has been successfully demonstrated for paramyxovirus (18). Although the signal to noise ratio is relatively modest, the small size of the MTRIPs and their ability to fluoresce at multiple wavelengths makes them a potential candidate for tracking virus RNA in living cells.

GFP-tagged mRNA

Viral mRNAs can be directly visualized while bound to GFP. In order to tag an mRNA, GFP is fused with an RNA- binding protein and expressed along with the target mRNA. A motif on the target mRNA is used to associate with the RNA binding protein (24). The coat protein of the bacteriophage MS2 has been identified as an ideal tag because it binds to a unique hairpin in genomic RNA with strong affinity (25). Using this approach, simultaneous imaging of the HIV-1 structural protein Gag and the HIV-1 genome has uncovered the dynamics and functional interactions during the packaging of

individual virions (26). A related study that employs simultaneous fluorescent imaging has shown that a few Gag molecules are required to recruit viral RNA into the plasma membrane (27). Both the reporter proteins and the target mRNA are genetically encoded; therefore, stable transgenic cell lines can be expressed and mRNA transport can be studied in detail. However, GFP tags might not have high multiplexing potential owing to the limited availability of high-affinity RNA tags and the contribution of high background fluorescence (24). Importantly, this approach is only suitable for studying the fundamental mechanisms of the viral life cycle, but not for clinical detection of viral infection.

Molecular beacons

For some viruses, like hepatitis A virus (HAV), the viral replication process is relatively slow and non-lytic; as such, cultivation in the laboratory could take up to several weeks for maximum virus production (28). This presents a significant challenge to detect infectious viruses that rely on the visualization of cytopathic effects (CPE) using mammalian cell culture method. Therefore, rapid methods are needed to better understand the replication cycle and for early detection of viral infection. Molecular beacons (MBs) are single-stranded oligonucleotide probes that form a stem-loop structure with a fluorophore at the 5' end and a quencher at the 3' end (Figure 1.1.) (29-31). Upon excitation of the fluorophore, energy is transferred to the quencher through a process called fluorescence resonance energy transfer (FRET), resulting in a loss of fluorescence signal. However, in the presence of a complementary target, the fluorophore and the

quencher move apart in response to a spontaneous conformational change, thus allowing the MB to fluoresce as a direct indicator of target binding (Figure 1). The spontaneous hybridization that occurs between the beacon and the target is highly specific and can be used to differentiate even a single base pair mismatch (32-34). Using this technique, a combined cell culture-MB assay was reported for the detection of HAV by visualizing the viral RNA in infected cells after permeabilization (28).

The use of MBs to provide a dynamic snapshot of the translocation of PV RNA has also been demonstrated, which indicates the potential to conduct transient studies inside infected cells (35). A similar success has been achieved by probing the intracellular transport of influenza virus mRNA in infected cells (36). Results indicate that influenza virus mRNA transport is energy-dependent by utilizing the cellular TAP/p15 transport pathway with the participation of the viral NS1 protein and cellular RNAP-II. The possibility of studying the spread of bovine respiratory syncytial virus (bRSV) in living cells over a 7-day period has also been demonstrated (37). Unfortunately, no real-time information was provided as the MBs were introduced only at different post-infection time points, rather than immediately following infection.

Improved MBs for imaging viral replication in live cells

Even though MBs have enabled live-cell imaging, some of the major challenges in using traditional MBs for *in vivo* imaging include their modest half-life (~50 min) owing to nuclease degradation and the lack of a non-invasive intracellular delivery technique (38,39). The stability of MBs can be improved significantly by modifying the

oligonucleotide backbones using 2'-*O*-methyl RNA bases and 2'-*O*-methyl-phosphorothioate internucleotide linkages (40). To provide non-invasive delivery of MBs across the plasma membrane, the pore-forming bacterial exotoxin, SLO, has shown promise as a potential delivery tool. However, some studies report rapid nuclear localization of cargoes. Moreover, it can only be used in *ex vivo* cellular assays (41). The HIV-1-derived TAT peptide is a cell-penetrating carrier that has received attention as a possible vector for the delivery of oligonucleotides across the cell membrane in a seemingly energy-independent manner (42-44). The TAT-based delivery method does not interfere with specific targeting or produce hybridization-induced fluorescence of the MBs (45). This novel delivery method, when combined with nuclease resistant MBs, can provide real-time monitoring of coxsackievirus B6 virus replication in living cells as well as intercellular spreading of infection (14). These results suggest that the TAT-modified, nuclease-resistant MBs might be very useful for understanding the dynamic behavior of viral replication and for therapeutic studies of anti-viral treatments.

Another major limitation to conventional MBs for FRET-based applications is the use of organic fluorophores that have low resistance to photo degradation, making them unsuitable for long-term *in vivo* imaging (46). Semiconductor nanocrystals known as quantum dots (QD) have gained a lot of attention for viral imaging applications owing to their excellent photo stability, brighter fluorescence than organic fluorophores, and their ability to be used in multiplex detection schemes (46-47). A study was reported for the development of nuclease-resistant MBs using QD and Au NPs as the FRET pair (48-50), (44) for real-time *in vivo* viral detection via TAT peptide delivery. The new FRET pair

(Au-NP–MB) resulted in a 7-fold increase in fluorescent signal upon target binding, making it suitable for exploring the real-time molecular mechanisms that are essential for viral pathogenesis (51).

Fluorescence labeling methods for visualizing viral infection

In addition to probing viral RNA for real-time monitoring of viral infection, other viral replication events inside a host cell can be exploited for non-invasive detection. One popular and powerful method involves single-virus tracking in living cells. Single-virus tracking incorporates live-cell imaging of cells infected with recombinant viruses expressing fluorescently tagged structural viral proteins and cellular structures of interest (52). This method enables the dynamic visualization of the virus maturation pathways at a single virus-particle level. A crucial requirement of this technique involves labeling of both viruses and cellular structures with a sufficient number of fluorophores for detection, without inhibiting viral infectivity and cell functions. Two general strategies exist for labeling viruses: the fusion of a target viral protein with a fluorescent protein (FP), or direct chemical labeling with a small fluorescent dye (52).

Fluorescent protein tagging

To incorporate a FP, the DNA sequence of the FP is inserted into the open reading frame of the target viral protein; labeling then occurs during virus replication in host cells. FP labeling has been used to study the dynamics of virus entry (15), (52-53) to distinguish between complete and subviral particles after membrane fusion (54), and to visualize the replication cycle of viruses (55). Unfortunately, studying viral assembly is often difficult using FPs because fluorescent viral proteins are usually overexpressed in an infected cell, resulting in a considerable amount of background signal. However various approaches including instrumentation (2 photon laser scanning microscopy, time

resolved fluorescence microscopy), chemical methods (auto fluorescence quenching) and molecular approaches (different mutants, promoters, varying ratio of wild type and FP) can be used to increase signal to noise ratio (56).

Chemical labeling

Viral structures can be chemically labeled in purified form and used for viral entry, transport, assembly; and can also be labeled using specific dyes after infection to study replication (52). Chemical labels (CLs) can be either covalently attached or non-covalently associated with the target protein. For example, capsids of purified, non-enveloped viruses can be covalently labeled with amino-reactive dyes (e.g. Alexa) (52), whereas the outer membrane of purified enveloped viruses can be labeled with lipophilic dyes and analogues (57). Although labeling of viral structural proteins enables the tracking of individual virus particles in living cells, there are certain limitations. Firstly, due to the smaller structure of the viruses, a limited number of fluorescent CLs can be attached to a virus particle without causing self-quenching effects or affecting viral infectivity (57). Secondly, as the cells also fluoresce, it can be difficult to distinguish between the signal from a single virus particle and the background fluorescence of a cell; however, the use of red fluorescent dyes, such as Cy5, Alexa 647, and 1,1'-dioctadecyl-3,3,3',3'-tetramethylindodicarbocyanine perchlorate (DiD) and red fluorescent proteins, such as mCherry, can be used to negate the background signal problem, as the cell auto-fluorescence background levels tend to be weaker at longer excitation wavelengths.

Interestingly, metabolic labeling can be used to label viruses during viral replication. This approach uses cell-permeable biarsenical dyes, which can specifically bind to viral proteins that contain tetracysteine (TC) peptide sequences. A small tetracysteine tag containing two pairs of cysteines held in a hairpin configuration (e.g. CCPGCC) can be genetically engineered into the protein of interest (58), which then specifically reacts with membrane-permeable biarsenical compounds that selectively fluoresce when covalently bound to the cysteine pairs. This genetic tag is relatively small and simple; thus, it can be placed into target proteins with minimal disruption. Furthermore, the cysteine-based structure can form even under detergent-based denaturing conditions, indicating that the dye-binding sequence does not require extensive structure for activity (58). Therefore, the TC tag is competent to bind biarsenical dyes almost immediately after translation and can fluoresce more rapidly.

An additional advantage is the availability of two colors of biarsenical reagents, FlAsH and ReAsH, which fluoresce green and red, respectively. This allows for examining the accumulation of nascent protein by labeling the existing target protein in the cell with one color and then labeling newly synthesized protein with the other (58). This approach has been used to examine the localization of HIV-1 Gag inside cells, and to identify the trafficking patterns of newly synthesized Gag by fluorescently labeling HIV-1 Gag (59). As an additional example, the challenge of generating replication-competent fluorescent influenza A virus is its segmented genome; this was overcome by introducing the TC biarsenical labeling system into influenza virus in order to fluorescently label viral protein in the virus life cycle (60). With biarsenical labeling, the

engineered replication-competent virus allowed the real-time visualization of nuclear import of the NS1 protein, which is involved in multiple functions during virus infection. These results establish biarsenical labeling as an important method to study viral protein-host factor interactions during virus infection.

Good photo stability of fluorophore labels is desirable for the continuous tracking of individual viruses. QDs are ideal for single-virus trafficking and imaging because they exhibit remarkable photo stability (retains 97% of initial intensity compared to 55% for organic dyes at the end of 3 min of illumination) (61) and brightness (molar extinction coefficients is 10–100✕ that of organic dyes) (62). Successful examples of tagging viruses with QDs include: (i) the use of 2-3 antibody layers (a virus-specific primary antibody, followed by a biotin-labeled secondary antibody and a streptavidin-conjugated QD) (47),(63); (ii) encapsulation of QDs in viral capsids (64); and (iii) covalent linkage of QDs to viral capsids (65-66). However, these labeling schemes likely affect the normal properties of viruses as well as their interactions with the host (52). Thus, a new general method to site-specifically label live and membrane-enveloped viruses using QDs was developed (12). The strategy was to first incorporate a 15-amino-acid biotin acceptor peptide tag onto the surface of a virion, followed by modifying the peptide tag with biotin ligase to introduce the biotin moiety to the viral surface. By means of the tight interaction between biotin and streptavidin ($K_d = 10^{-13}$ M), the addition of streptavidin-conjugated QDs allowed the site-specific labeling of viral particles with QDs. The authors were able to study the kinetics of internalization of the recombinant lentivirus enveloped with vesicular stomatitis virus glycoprotein into the early endosomes (12) and also perform

live-cell imaging of viral trafficking to the Rab5$^+$ endosomal compartments. The utility

of this technique was further demonstrated to study the molecular mechanisms of viral

entry. The enhanced brightness of QD-labeled HIV particles has enabled the detection of

single virions on the surface of target cells expressing either CD4/CCR5 or DC-SIGN

(12) and a detailed tracking of the viral internalization. These studies exhibit the potential

of QD based probes for visualizing viral and host structure interactions.

Viral proteases as the probing target

For many viruses the introduction of thousands of virus particles is required to

infect a single cell, making it difficult to track an infectious versus non-infectious virus

particle (67). Viruses, such as picornaviruses, retroviruses, and caliciviruses, however,

produce a polyprotein that is cleaved into individual proteins by virus-specific proteases.

Thus, viral proteases could be a prime target for the detection of viral infection because

within various viral families the proteolytic cleavage event proceeds in a defined manner

for production of infectious virus particles.

Immediately upon infection, the RNA genome is translated into a single

polypeptide, which is subsequently cleaved by viral proteases to generate mature viral

proteins with high efficiency and specificity. Currently, to monitor the proteolytic event

inside a host cell, one must engineer a FP pair linked by the target protease sequence of

interest. Proteolytic cleavage of the target sequence can therefore be detected based on

changes in the FRET using high-resolution live-cell imaging (68). Several FRET reporter

cell lines expressing various FP pairs, such as CFP-YFP (69) and EGFP-DsRed2 (70),

have been designed. FRET-based assays have been used for the rapid detection (within

7.5 h) of very low doses of infectious enteroviruses (≤10 PFU) (69). In addition, the FP

pair can be used to probe the dynamic distribution of enterovirus protease in living cells

(70). Although most of the FRET analyses have been performed using fluorescence

microscopy, flow cytometry has recently been used to provide automated analysis of

fluorescent cells for rapid detection of viral infection and enumeration of infected cells

(71). However, the biggest challenge of this method is the development of a stable clone

expressing the fluorescent substrate for each protease, which is a time-consuming and

intensive task because considerable optimization is required for the development of each

stable clone. An alternative would be to deliver a synthetic FRET substrate carrying the

specific proteolytic site of each protease into living cell using cell penetrating peptides

(72).

QD based FRET probes

One major limitation of conventional FRET substrates is the use of either organic

fluorophores or FPs as the label, which exhibit low resistance to photo degradation. As

described in the earlier sections, QDs have the potential to circumvent these limitations

owing to their excellent physical and optical properties. Recently, FRET-based bioassays

have been successfully demonstrated using QDs as the energy donor and fluorescent dyes

or quenchers as energy acceptors (72). In addition, QDs attached to FPs have been

successfully delivered into cells by using cell penetrating peptides, such as TAT (73).

This novel delivery method, when combined with protease-specific FRET pairs, could

provide a powerful means for rapid, real-time detection of viral protease activity in living cells with high specificity and sensitivity. The feasibility of this approach was recently demonstrated by generating a QD-modified, protease-specific protein module that can be used as a FRET substrate for probing *in vivo* HIV-1 protease activity (74).

References

1. Namendys-Silva, S. A., E. Rivero-Sigarroa, and G. Dominguez-Cherit. 2010. Acute Respiratory Distress Syndrome Induced by Pandemic H1N1 2009 Influenza A Virus Infection. *Am. J. Respir. Crit. Care Med.* 182: 41-48.

2. Su, J. R. 2004. Emerging viral infections. *Clin. Lab. Medicine.* 24:773-795.

3. Moore, C. L., J. A. Smagala, C. B. Smith, E. D. Dawson, N. J. Cox, R. D. Kuchta, and K. L. Rowlen. 2007. Evaluation of MChip with Historic Subtype H1N1 Influenza A Viruses, Including the 1918 "Spanish Flu" Strain. *J. Clin. Microbiol.* 45:3807-3810.

4. Henrickson, K. J. 2004. Advances in the laboratory diagnosis of viral respiratory disease. *Pediatr. Infect. Dis. J.* 23:S6-S10.

5. Mahy, B. W. J., and H. O. Kangro, 1996. *Virology methods manual*. Academic press, 3-144.

6. Parida, M. M. 2008. Rapid and real-time detection technologies for emerging viruses of biomedical importance. *J. Biosciences.* 33:617-628.

7. Marsh, M., and A. Helenius. 2006. Virus entry: Open sesame. *Cell.* 124:729-740.

8. Greber, U. F., and M. Way. 2006. A superhighway to virus infection. *Cell.* 124:741-754.

9. Whittaker, G. R., and A. Helenius. 1998. Nuclear import and export of viruses and virus genomes. *Virology.* 246:1–23.

10. Stidwill, R. P., and U. F. Greber. 2000. Intracellular Virus Trafficking Reveals Physiological Characteristics of the Cytoskeleton. *News physiol. sci.* 15:67-71.

11. Sattentau, Q. J. 2010. Cell-to-Cell Spread of Retroviruses. *Viruses.* 2:1306-1321.

12. Joo, K. I., Y. Lei, C.-L. Lee, J. Lo, J. Xie, S. F. Hamm-Alvarez, and P. Wang. 2008. Site-specific labeling of enveloped viruses with quantum dots for single virus tracking. *Acs Nano.* 2:1553-1562.

13. Pan, K.-L., J.-C. Lee, H.-W. Sung, T.-Y. Chang, and J. T.-A. Hsu. 2009. Development of NS3/4A Protease-Based Reporter Assay Suitable for Efficiently Assessing Hepatitis C Virus Infection. *Antimicrob. Agents Ch.* 53:4825-4834.

14. Yeh, H.-Y., M. V. Yates, A. Mulchandani, and W. Chen. 2008. Visualizing the dynamics of viral replication in living cells via Tat peptide delivery of nuclease-resistant molecular beacons. *Proc. Natl. Acad. Sci. U.S.A.* 105:17522-17525.

15. Brandenburg, B., L. Y. Lee, M. Lakadamyali, M. J. Rust, X. Zhuang, J. M. Hogle. 2007. Imaging poliovirus entry in live cells. *Plos Biol.* 5:1543-1555.

16. Lakadamyali, M., M. J. Rust, H. P. Babcock, and X. Zhuang. 2003. Visualizing infection of individual influenza viruses. *Proc. Natl. Acad. Sci. U.S.A.* 100:9280-9285.

17. Campbell, E. M., and Hope, T. J. 2008. Live cell imaging of the HIV-1 life cycle. *Trends Microbio.* 16:580-587.

18. Santangelo, P. J., A. W. Lifland, P. Curt, Y. Sasaki, G. J. Bassell, M. E. Lindquist, and J. E. Crowe Jr. 2009. Single molecule-sensitive probes for imaging RNA in live cells. *Nat. Methods.* 6:347-349.

19. Fusco, D., E. Bertrand, and R. H. Singer. 2003. Imaging of Single mRNAs in the Cytoplasm of Living Cells. In *RNA Trafficking and Nuclear Structure Dynamics*. (Jeanteur, P., eds), pp. 135-150, Springer.

20. Scull, M. A., and C. M. Rice. 2010. A big role for small RNAs in influenza virus replication. *Proc. Natl. Acad. Sci. U.S.A.* 107:11153-11154.

21. Burton, M. V., R. M. McCullough, C. R. Cantor, and N. E. Broude1. 2007. RNA visualization in live bacterial cells using fluorescent protein complementation. *Nat. Methods. 4*:421-427.

22. Politz, J. C. 1999. Use of caged fluorochromes to track macromolecular movements in living cells. *Trends Cell Biol.* 9:284-287.

23. Beach, D. L., E. D. Salmon, and K. Bloom. 1999. Localization and anchoring of mRNA in budding yeast. *Curr. Biol.* 9:569-578.

24. Tyagi, S. 2009. Imaging intracellular RNA distribution and dynamics in living cells. *Nat. Methods*. 6:331-338.

25. Bertrand, E., P. Chartrand, M. Schaefer, S. M. Shenoy, R. H. Singer, and R. M. Long. 1998. Localization of ASH1 mRNA particles in living yeast. *Mol. Cell.* 2:437-445.

26. Fusco, D., N. Accornero, B. Lavoie, S. M. Shenoy, J.-M. Blanchard, R. H. Singer, and E. Bertrand. 2003. Single mRNA molecules demonstrate probabilistic movement in living mammalian cells. *Curr. Biol*. 13:161-167.

27. Jouvenet, N., S. M. Simon, and P. D. Bieniasz. 2009. Imaging the interaction of HIV-1 genomes and Gag during assembly of individual viral particles. *Proc. Natl. Acad. Sci. U.S.A.* 106:19114-19119.

28. Yeh, H.-Y., Y.-C. Hwang, M. V. Yates, A. Mulchandani, and W. Chen. 2008. Detection of hepatitis A virus using a combined cell culture-molecular beacon assay. *Appl. Environ. Microbiol.* 74:2239-2243.

29. Tyagi, S., and F. R. Kramer. 1996. Molecular beacons: probes that fluoresce upon hybridization. *Nat. Biotechnol.* 14:303-308.

30. Drake, T. J., and W. Tan. 2004. Molecular beacon DNA probes and their bioanalytical applications. *Appl. Spectrosc.* 58:269-280.

31. Goel, G., A. Kumar, A. K. Puniya, W. Chen and K. Singh. 2005. Molecular beacon: a multitask probe. *J. Appl. Microbiol.* 99:435-442.

32. Marras, S. A. E., F. R. Kramer, and S. Tyagi. 1999. Multiplex detection of single-nucleotide variations using molecular beacons. *Genet. Anal-Biomol. E.* 14:151-156.

33. Tyagi, S., D. P. Bratu, and F. R. Kramer. 1997. Multicolor molecular beacons for allele discrimination. *Nat. Biotechnol.* 16:49-53.

34. Tyagi, S., and O. Alsmadi. 2004. Imaging native β-actin mRNA in motile fibroblasts. *Biophys.* 87:4153-4162.

35. Cui, Z.-Q., Z.-P. Zhang, X.-E. Zhang, J.-K. Wen, Y.-F. Zhou, and W.-H. Xie. 2005. Visualizing the dynamic behavior of poliovirus plus-strand RNA in living host cells. *Nucleic Acids Res.* 33:3245-3252.

36. Wang, W., Z.-Q. Cui, H. Han, Z.-P. Zhang, H.-P. Wei, Y.-F. Zhou, Z. Chen, and X.-E. Zhang. 2008. Imaging and characterizing influenza A virus mRNA transport in living cells. *Nucleic Acids Res.* 36:4913-4928.

37. Santangelo, P., N. Nitin, L. LaConte, A. Woolums, and G. Bao1. 2005. Live-cell characterization and analysis of a clinical isolate of bovine respiratory synctial virus using molecular beacons. *J. Virol*. 80:682-688.

38. Bratu, D. P., B. J. Cha, M. M. Mhlanga, F. R. Kramer, and S. Tyagi. 2003. Visualizing the distribution and transport of mRNA in living cells. *Proc. Natl. Acad. Sci. USA*. 100:13308-13313.

39. Cotten, M., B. Oberhauser, H. Brunar, A. Holzner, G. Issakides, C. R. Noe, G. Schaffner, E. Wagner, and M. L. Birnstiel. 1991. 2'-O-methyl, 2'-O-methyl oligoribonucleotides and phosphorothioate oligodeoxyribonucleotides as inhibitors of the *in vitro* U7 snRNP-dependent mRNA processing event. *Nucleic Acids Res*. 19:2629-2635.

40. Chen, A., M. A. Behlke, A. Tsourkas. 2009. Sub-cellular trafficking and functionality of 2'-O-methyl and 2'-O-methyl-phosphorothioate molecular beacons. *Nucleic Acids Res.* 37:*e149.*

41. Spiller, D. G., R. V. Giles, J. Grzybowski, D. M. Tidd, and R. E. Clark. 1998. Improving the intracellular delivery and molecular efficacy of antisense oligonucleotides in chronic myeloid leukemia cells: a comparison of streptolysin-O permeabilization, electroporation and lipophilic conjugation. *Blood.* 91:4738-4746.

42. Deshayes, S., M. C. Morris, G. Divita, F. Heitz..2005. Cell-penetrating peptides: tools for intracellular delivery of therapeutics. *Cell Mol. Life Sci*. 62:1839-1849.

43. Kueltzo, L. A., and C. R. Middaugh. 2000. Potential use of non-classical pathways for the transport of macromolecular drugs. *Expert Opin. Invest Drugs*. 9:2039-2050.

44. Saalik, P., A. Elmquist, M. Hansen, K. Padari, K. Saar, K. Viht, U. Langel, and M. Pooga. 2004. Protein cargo delivery properties of cell-penetrating peptides. A comparative study. *Bioconjug. Chem*. 15:1246-1253.

45. Nitin, N., P. J. Santangelo, G. Kim, S. Nie and G. Bao. 2004. Peptide-linked molecular beacons for efficient delivery and rapid mRNA detection in living cells. *Nucleic Acids Res.* 32:e58.

46. Goldman, E. R., G. P. Anderson, P. T. Tran, H. Mattoussi, P. T. Charles, J. M. Mauro. 2002. Conjugation of luminescent quantum dots with antibodies using an engineered adaptor protein to provide new reagents for fluoroimmunoassays. *Anal. Chem*. 74:841-847.

47. Michalet, X., F. F. Pinaud, L. A. Bentolila, J. M. Tsay, S. Doose, J. J. Li, G. Sundaresan, A. M. Wu, S. S. Gambhir, and S. Weiss. 2005. Quantum dots for live cells and *in vivo* imaging, diagnostics and beyond. *Science.* 307:538-544.

48. Dubertret, B., M. Calame, and A. J. Libchaber. 2001. Single-mismatch detection using gold-quenched fluorescent oligonucleotides. *Nat. Biotechnol.* 19:365-370.

49. Dyadyusha, L., H. Yin, S. Jaiswal, T. Brown, J. J. Baumberg, F. P. Booy and T. Melvin. 2005. Quenching of CdSe quantum dot emission, a new approach for biosensing. *Chem. Commun*. 3201-3203.

50. Pons, T., I. L. Medintz, K. E. Sapsford, S. Higashiya, A. F. Grimes, D. S. English, and H. Mattoussi. 2007. On the quenching of semiconductor quantum dot photoluminescence by proximal gold nanoparticles. *Nano Lett.* 7:3157-3164.

51. Yeh, H.-Y., M. V. Yates, A. Mulchandani, and W. Chen. 2010. Molecular beacon-quantum dot- Au nanoparticle hybrid nanoprobes for visualizing virus replication in living cells. *Chem. Commun.* 46:3914-3916.

52. Bradenburg, B., and X. Zhuang. 2007. Virus Trafficking − Learning from Single-Virus Tracking. *Nat. Rev. Microbiol.* 5:197-208.

53. Koch, P., M. Lampe, W. J. Godinez, B. Muller, K. Rohr, H.-G. Krausslich, and M. J. Lehmann. 2009. Visualizing fusion of pseudotyped HIV-1 particles in real time by live cell microscopy. *Retrovirology.* 6:84.

54. Lampe, M., J. A. Briggs, T. Endress, B. Glass, S. Riegelsberger, H. G. Krausslich, D. C. Lamb, C. Brauchle, B. Muller. 2007. Double-labeled HIV-1 particles for study of virus–cell interaction. *Virology*. 360:92-104.

55. Shi, X., J. T. van Mierlo, A. French, R. M. Elliott. 2010. Visualizing the Replication Cycle of Bunyamwera Orthobunyavirus Expressing Fluorescent Protein-Tagged Gc Glycoprotein. *J. Virol.* 84:8460–8469.

56. Billinton, N., and A. W. Knight. 2001. Seeing the Wood through the Trees: A Review of Techniques for Distinguishing Green Fluorescent Protein from Endogenous Autofluorescence. *Anal. Biochem.* 291:175-307.

57. Seisenberger, G., M. U. Ried, T. Endre, H. Buning, M. Hallek, and C. Brauchle. 2001. Real-time single-molecule imaging of the infection pathway of an adeno-associated virus. *Science.* 294:1929–1932.

58. Adams, S. R., R. E. Campbell, L. A. Gross, B. R. Martin, G. K. Walkup, Y. Yao, J. Llopis, and R. Y. Tsien. 2002. New biarsenical ligands and tetracysteine motifs for protein labeling in vitro and in vivo: synthesis and biological applications. *J. Am. Chem. Soc.* 124:6063-6076.

59. Rudner, L. S., S. Nydegger, L. V. Coren, K, Nagashima, M. Thali, and D. E. Ott. 2005. Dynamic fluorescent imaging of human immunodeficiency virus type 1 Gag in live cells by biarsenical labeling. *J. Virol.* 79:4055-4065.

60. Li, Y., X. Lu, J. Li, N. Berube, K. L. Giest, Q. Liu, D. H. Anderson, Y. Zhou..2010. Genetically Engineered, Biarsenically Labeled Influenza Virus Allows Visualization of Viral NS1 Protein in Living Cells. *J. Virol.* 84:7204-7213.

61. Wu, X., H. Liu, J. Liu, K. N. Haley, J. A. Treadway, J. P. Larson, N. Ge, F. Peale, and M. P. Bruchez. 2002. Immunofluorescent labeling of cancer marker Her2 and other cellular targets with semiconductor quantum dots. *Nat. Biotechnol.* 21:41 - 46.

62. Medintz, I. L., H. T. Uyeda, E. R. Goldman, and H. Mattoussi. 2005. Quantum dot bioconjugates for imaging, labeling and sensing. *Nat. Mater.* 4:435 - 446.

63. Bentzen, E. L., F. House, T. J. Utley, J. E. Crowe Jr, and D. W. Wright. 2005. Progression of Respiratory Syncytial Virus Infection Monitored by Fluorescent Quantum Dot Probes. *Nano Lett.* 5:591-595.

64. Dixit, S. K., N. L. Goicochea, M.-C. Daniel, A. Murali, L. Bronstein, M. De, B. Stein, V. M. Rotello, C. C. Kao, and B. Dragnea. 2006. Quantum Dot Encapsulation in Viral Capsids. *Nano Lett*. 6:1993-1999.

65. Agrawal, A., R. A. Tripp, L. J. Anderson, and S. Nie. 2005. Real-Time Detection of Virus Particles and Viral Protein Expression with Two-Color Nanoparticle Probes. *J. Virol.* 79:8625-8628.

66. Chen, Y. H., C. H. Wang, C. W. Chang, C. A. Peng. 2010. In situ formation of viruses tagged with quantum dots. *Integr. Biol (Camb).* 2:258-64.

67. Carpenter, J. E., E. P. Henderson, and C. Grose. 2009. Enumeration of an Extremely High Particle-to-PFU Ratio for Varicella-Zoster Virus. *J. Virol.* 83:6917-6921.

68. Jares-Erijman, E. A., and T. M. Jovin. 2003. FRET imaging. *Nat. Biotechnol.* 21:1387–1395.

69. Hwang, Y. C., W. Chen, M. V. Yates. 2006. Use of fluorescence resonance energy transfer for rapid detection of enteroviral infection in vivo. *Appl. Environ. Microbiol.* 72:3710–3715.

70. Hsu, Y. Y., Y.-N. Liu, W. Wang, F.-J. Kao, S.-H. Kung. 2007. In vivo dynamics of enterovirus protease revealed by fluorescence resonance emission transfer (FRET) based on a novel FRET pair. *Biochem. Biophys. Res. Commun.* 353:939–945.

71. Cantera, J. L., W. Chen, and M. V. Yates. 2010. Detection of infective poliovirus by a simple, rapid, and sensitive flow cytometry method based on fluorescence resonance energy transfer technology. *Appl. Environ. Microbiol.* 76:584-588.

72. Medintz, I. L., A. R. Clapp, F. M. Brunel, T. Tiefenbrunn, H. T. Uyeda, E. L. Chang, J. R. Deschamps, P. E. Dawson, and H. Mattoussi. 2006. Proteolytic activity monitored by fluorescence resonance energy transfer through quantum-dot–peptide conjugates. *Nat. Mater.* 5:581-589.

73. Medintz, I. L., T. Pons, J. B. Delehanty, K. Susumu, F. M. Brunel, P. E. Dawson, and H. Mattoussi. 2008. Intracellular Delivery of Quantum Dot-Protein Cargos Mediated by Cell Penetrating Peptides. *Bioconjugate Chem.* 19:1785–1795.

74. Biswas, P., L. N. Cella, S. H. Kang, A. Mulchandani, M. V. Yates and W. Chen. 2011. A quantum-dot based protein module for in vivo monitoring of protease activity through fluorescence resonance energy transfer. *Chem. Commun.* 47: 5259-5261.

Legends to Figures

Fig.1.1. Schematic representation of the molecular beacon and its application in live-cell tracking and imaging of viral RNA. The molecular beacons (MBs) form a closed hairpin structure in the absence of a complementary target. The proximity of the quencher (3') to the fluorophore (5') results in a loss of fluorescence signal. In the presence of a complementary viral RNA target, the MB opens up; this can be directly measured as a fluorescent signal. MBs are introduced into live cells to visualize viral RNA. Hybridization with complementary target RNA results in a direct fluorescent signal which is observed at different stages of viral infection.

Fig. 1.1.
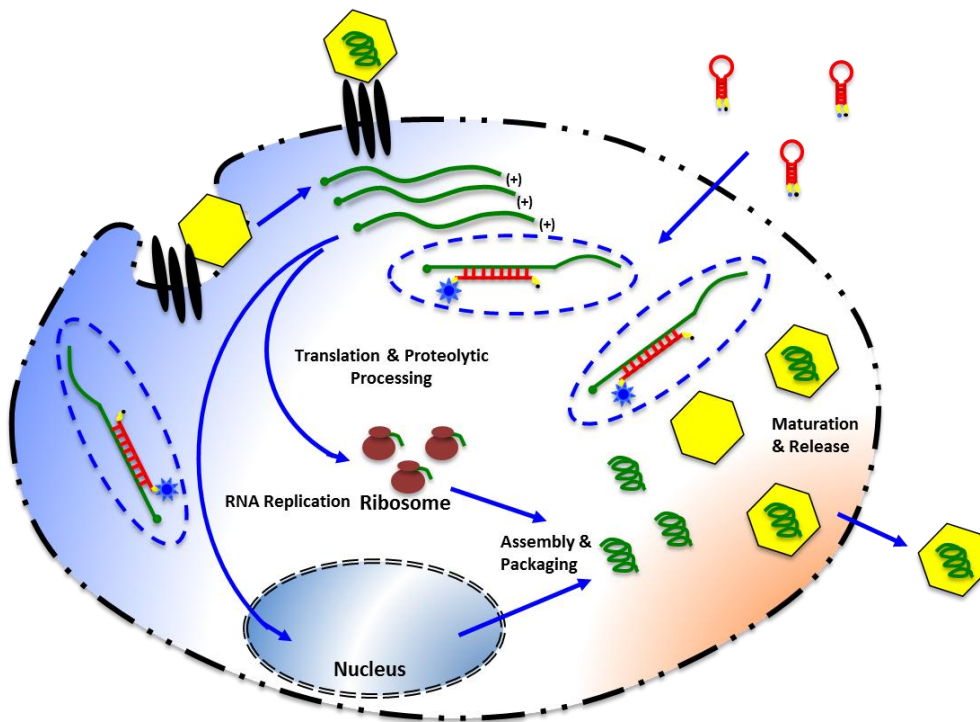
Chapter 2

Detection of infective poliovirus by a simple, rapid and sensitive flow cytometry method using molecular beacons

Abstract

Rapid and efficient detection of viral infection is crucial for the prevention of disease spread during an outbreak and timely clinical management. Some conventional techniques that have been developed for this purpose include immunofluorescence and serological methods. An alternative approach has been studied that utilizes a nuclease-resistant molecular beacon (MB) to specifically target a 20-bp 5' noncoding region of poliovirus-1 to detect the presence of the virus. A cell-penetrating Tat peptide was conjugated to the MB for intracellular delivery. Buffalo green monkey kidney (BGMK) cell monolayers were infected with varying titres of poliovirus-1(PV1) and the Tat conjugated beacons were introduced to detect the presence of infected cells. The fluorescent signal from MBs upon hybridizing with the viral mRNA was visualized using a fluorescence microscope. To demonstrate the flexibility of this technique to be adapted into a high-throughput screening method, a flow cytomtery (FC) based system was utilized and the simplicity of using a flow based scheme for rapid identification of infected cells was demonstrated. The sensitivity of the assay to detect less than 1% infected cells in a mixed cell population was shown. The illumination of fluorescent cells increased in a dose-responsive manner and enabled direct quantification of infectious viral doses. Fluorescent signal from virus infected cells was discernible as early as 15 min thereby enabling rapid detection. This approach is therefore more rapid than plaque assay and can be easily adapted to detect other epidemiologically more important viruses.

Introduction

Rapid detection of infective viruses is of great importance in the field of biomedicine and biotechnology. Viruses are causative agents for various human diseases and it is crucial to gather information on viral nucleic acids, life cycles and mode of infection. This knowledge will allow us in advancing the development of vaccines and therapies to treat and prevent viral infection (1). The current methods that are being employed to detect and study viruses have their share of benefits and limitations. Conventional techniques such as cell culture that rely on the production of cytopathic effect (CPE) are time consuming and laborious. Antibodies have been widely used to detect viral proteins (2) but because of their specificity, they must be generated and optimized for every target thereby making them unsuitable as a rapid detection technique. Techniques such as immunofluorescence and enzyme linked immunosorbent assay (ELISA) have also been used for viral particle detection, although they suffer from poor sensitivity and specificity, making it difficult to interpret the results (3). Hence development of improved methods for rapid, reliable detection and quantification of infectious viruses is necessary.

For this study, we utilized molecular beacons that have now been employed for over a decade for various applications such as in vitro hybridization assays (4-6), RNA imaging (7) and real time detection of DNA-RNA hybridization in living cells (8). Molecular beacons (MBs) are single-stranded oligonucleotide probes that form a stem–loop structure and are doubly labeled with a fluorophore at the 5' end and a quencher at

the 3' end (9). Upon excitation of the fluorophore, energy is transferred to the quencher through a process called fluorescence resonance energy transfer (FRET), which results in loss of the fluorescence signal (Figure 2.1.). However, in the presence of a complementary target, the fluorophore and the quencher move apart in response to a spontaneous conformational change, thus allowing the MB to fluoresce as a direct indicator of target binding. The spontaneous hybridization that occurs between the beacon and the target is highly specific and can be used to differentiate even a single base pair mismatch (10-12). Although MBs have been commonly used for intracellular detection of gene expression, their applications for the *in vivo* detection of viral RNA have been reported only recently (13). Some of the major challenges in using conventional MBs for *in vivo* viral detection are their susceptibility to nuclease degradation and a lack of non-invasive delivery method. Recently, the use of nuclease-resistant, MBs for the real-time detection of coxsackievirus replication in living cells via Tat peptide delivery has been successfully demonstrated (14). One can easily envision an extension of this technique as a diagnostic tool to detect the presence of virus- infected cells. While fluorescence microscopy can be used to visualize infected cells, an automated platform is required to provide quantitative information to systematically monitor and characterize the propagation of the virus in mammalian cells.

Flow cytometry represents a platform for rapid and high-throughput detection of infected cells from a large cell population. The use of flow cytometry to monitor viral infection and determine the viral titres has been previously reported for different types of viruses (15-19). However, those methods are laborious as they involve multiple steps

such as cell fixation, permeabilization, labeling and washing. Here we utilize a simple system that requires no cell pre-treatment using MBs that provide a label-based and separation-free detection scheme. Poliovirus was used as a model virus to demonstrate this principle because it is a well-studied virus for several decades and offers safe working conditions.

Materials and Methods

BGMK cell culture

 Buffalo green monkey kidney (BGMK) cells were cultured in autoclavable Eagle's minimal essential medium (AMEM) with Earle's salts (Irvine Scientific, Santa Ana, CA) containing 0.075% $NaHCO_3$, 10mM nonessential amino acids (NEAA; Gibco BRL, Grand Island, NY), 2mM L-glutamine (Hyclone, Logan, UT), 20mM HEPES (pH 7.4), 100 mg/ml penicillin, 100U/ml streptomycin (Hyclone) and 8% (vol/vol) fetal bovine serum (FBS; Hyclone) and buffered with. Cells were grown in an incubator maintained at 37°C and 5% (vol/vol) CO_2. Phosphate-buffered saline solution (PBS; 0.01M phosphate, pH 7.4, 0.138 M Na Cl, and 2.7mM KCl) and Tris-buffered saline solution (TBSS; 0.05M Tris, pH 7.4, 0.28 M NaCl, 10mM KCl, and 0.82mM Na_2HPO_4) were used during the washing steps for BGMK cell culture.

Virus preparation

Poliovirus type 1(PV1) (strain LSc) was obtained from American Type Cell Culture (ATCC VR-59) and propagated in BGMK cells for upto 5 days at 37°C. The virus stock was harvested and purified by freeze-thaw method and extracting the cell lysate with chloroform (20). The fresh virus stock was stored as 500µl aliquots at -80°C until use.

Plaque assay

The PV1 virus stock was thawed and then a series of 10-fold serial dilutions in 1X PBS was prepared. BGMK cells that were 90% confluent and 1-day old and grown in 12-well, 22.1mm dishes (Costar; Corning) were infected with 1ml of virus dilution. After 90min of adsorption at room temperature, the solutions were aspirated and 1ml of 2% carboxymethylcellulose (CMC) sodium salt (Sigma-Aldrich) containing 100mL of 2X AMEM (Irvine Scientific) with 2mL of 7.5% $NaHCO_3$, 4mL of 1M Hepes, 2mL of NEAA, 5mL of A/B-L, and 4mL of FBS (Sigma-Aldrich) was added to each well. After 5 days of incubation at 37°C, the CMC layer was removed and the cells were stained and fixed with 0.8% crystal violet and 3.7% formaldehyde solution for 2 hours. The excess stain was removed by washing with de-ionized water and virus plaques were counted to calculate the titre of the stock.

Molecular beacon design

The MB PV1was configured from the sequences of poliovirus strains obtained from GenBank database. To study the thermodynamic properties and predict secondary structures of the MB, a DNA folding program *mfold* (www.bioinfo.rpi.edu) was used. The molecular beacon (MB-PV1) (5'- 6FAM – CgAgCg**CCCAAAgTAgTCggTTCCgC**C/thiol-dG/gCTCg - DABCYL-3') was designed to be perfectly complementary to a 20-bp region of the 5' noncoding region of the poliovirus genome. The beacon was synthesized possessing a 2'-O-methylribonucleotide backbone with phosphorothioate internucleotide linkages by TIB

Molbiol. The thiol group near the 3' end of the beacon is for conjugation with a maleimide group attached to the C terminus of the Tat peptide to form a thiol-maleimide linkage. The MB-PV1 was solubilized in 100mM Tris-HCl (pH 8.0) buffer containing 1mM $MgCl_2$ to make a stock concentration of 100μM and stored at -20°C as 50μl aliquots until use.

Peptide Design

The C terminal maleimide modified Tat peptide Tyr-Gly-Arg-Lys-Lys-Arg-Arg-Gln-Arg-Arg-Arg-N-CH_2CH_2-N-maleimide (Global Peptide) was mixed with MB-PV1 in the molar ratio of 1:1.5. The reaction was allowed to occur at room temperature in the dark for 2 h to form a stable thiol-maleimide bond. The Tat peptide-conjugated with MB-PV1 (MB-PV1-Tat) was aliquoted and stored at -20°C for experimental use.

Infection of BGMK with PV1

BGMK cells were grown in 8 well Lab-Tek Chamber slide (Thermo Scientific- NUNC) at 37°C in 5% CO_2 (vol/vol) until 90% confluent. After aspirating the incubation medium, the cell monolayer was washed twice with 1 X phosphate buffered saline solution (PBS) and incubated with different concentrations of PV1. The virus was allowed to adsorb to the cell surface for 30min at 37°C then the unbound virus particles are removed. The infection was allowed to proceed for 18hrs.

Delivery of Tat conjugated MB's into infected cells

After 18hr P.I., the incubation media in the PV1 infected BGMK cells was removed and replaced with 1 X Leibovitz L-15 medium (Invitrogen). The Leibovitz L-15 medium contains no phenol red and is a CO_2 independent media making it suitable to perform experiments using the fluorescence microscope. MB-PV1-Tat (2μM) was slowly added to the infected cells and incubated at 37°C in the dark for 30 min prior to imaging and flow cytometry analysis.

Flow cytometry analysis

After incubation, the medium was aspirated from the cell monolayer and replaced with 0.1% trypsin in 0.05% EDTA (GIBCO) to detach the cells. A solution containing 10% FBS in 1X Tris-buffered saline (TBS) was added to the detached cells to neutralize the trypsin. Cells were harvested using a low-speed centrifuge at 1500rpm for 5 min. They were resuspended in 1X TBS containing 3mM EDTA (pH 8.0) to avoid clustering. A portion of the sample was aliquoted to observe under the microscope while the rest was used for flow cytomtery analysis. Cells were sieved using a 35μm nylon mesh cell strainer (BD Biosciences) prior to flow cytomtery analysis. The cells were analyzed using the BD FACS Aria cell sorting system using a 407nm UV laser for GFP excitation and an emission filter of detection was 520/20nm. Data acquisition (10^5 events per sample) and analysis were performed using BD FACSDiva software.

Fluorescence microscopy and image processing

 A Zeiss Axiovert 40 CFL inverted microscope supplied with an HBO 50W/AC mercury lamp (for fluorescence) and a12-V, 35-W halogen lamp was used to perform live cell imaging. For each sample well, both phase contrast and fluorescent pictures were taken. Image acquisition and processing was carried out using the Image-Pro analysis software (Media Cybernetics). All settings for image capture were kept consistent and the exposure time for each sample was maintained throughout the course of the experiment.

Enumeration of fluorescent cells

To calculate the percentage the fluorescent cells, firstly multiple phase contrast images of each well were taken to count the total number of cells. Simultaneously, the number of fluorescent cells was counted within those frames using Image-Pro PLUS analysis software.

Results and Discussion

Detection of PV1 infected cells by flow cytometry

The preliminary studies were tailored to demonstrate the ability of the proposed MB method to accurately identify infected cells in a sample composed of a mixture of infected and uninfected cells. To simulate these conditions, BGMK cells were infected with a high dosage (10^5 PFU) of PV1 and the infection was allowed to proceed for 18hrs. After 18hr post infection (P.I.) cells were detached from the monolayer using trypsin and prepared by mixing populations of highly infected cells with uninfected cells to mimic different percentages of infection (1%, 2%, 5%, 10%, 20% and 100%). The uninfected cells and infected cell mixture was then mixed with 1μM Tat-modified, nuclease-resistant MBs and quantified using a flow cytometer. Cells were gated according to their size and granularity so as to include only intact cells. Figure 2.2. shows the representative histogram that was generated from flow cytometry (FC) analysis. The uninfected (control) cells showed an insignificant background signal indicating the absence of any false positive signal. More importantly, a two-log increase in the fluorescence intensity was observed for the highly infected sample because of the spontaneous hybridization of the MBs with the target viral RNA. The number of fluorescent cells increased with an increase in the percentage of infected cells in the mixture suggesting a clear correlation between fluorescent cells measured by flow cytomtery and the infected cells in the mixture (Figure 2.3.). This further validates that the fluorescence measured by the FC was a result of hybridization between the MB and the target viral mRNA. This result

demonstrates conclusively that the MB-FC assay can be used to distinguish infected cells from uninfected cells based on the changes in fluorescence. Further, the sensitivity of the assay was demonstrated as it was able to measure less than 1% infected cells in a population of infected and uninfected cells.

Comparison of flow cytometry based assay with fluorescence microscopy

To validate the sensitivity of the FC based assay, the experiment was repeated in a similar manner and the quantification of fluorescent cells was performed using a fluorescence microscope. Again, BGMK cells were infected with a high dosage (10^5 PFU) of PV1 as before. Samples were prepared by mixing populations of highly infected cells with uninfected cells to represent different percentages of infection. The uninfected cells and infected cell mixture was then mixed with 1μM Tat-modified, nuclease-resistant MBs and allowed to incubate for 30 min in the dark before starting image acquisition. A GFP channel (475nm/520nm) was used to visualize the fluorescent cells. Compared with uninfected cultures, (0% infection) where no fluorescent cells were present, an increase in the number of fluorescent cells was detected with the increase in the percentage of infected cells in the mixture. The fluorescent images were merged with DIC to confirm that the fluorescence observed was intracellular. Although, the numbers of fluorescent cells appear to be similar across different infection mixtures, the merged image provides a better interpretation, as the total number of BGMK cells in each image varies (Figure 2.4.). As expected, for the 100% infected sample, nearly 100% of the cells were brightly

fluorescent, however the true merit of this technique was appreciated only while analyzing samples containing as low as 1% infected cells. The sensitivity of this method to capture a very few infected cells in a mixed population is especially useful in the field of disease diagnosis. To provide a quantitative comparison between FC based method and fluorescence microscopy, GFP fluorescence and DIC images were acquired for each of the different infection mixtures using the Image-Pro PLUS software. The total number of BGMK cells was counted in the DIC image and correspondingly the total number of fluorescent cells was counted for the same image to calculate the percentage of infected cells. In Figure 2.5., a direct comparison between the percentage of fluorescent cells counted from FC assay and fluorescent microscope is shown. A linear relationship was observed between the two assays indicating that the FC-based assay can accurately quantify the percentage of infected cells. While the fluorescence microscope based assay is useful for a qualitative understanding of the system and visualizing virus infected cells, the FC based assay provides a high-throughput and rapid flow based detection system.

Quantification of infectious PV1 dosage

In order to use this technique as a diagnostic tool, it is important to demonstrate the ability of this method to detect very low infectious dosages of the virus. To determine if the system could detect as few as 1 PFU, BGMK cells were infected with varying dosage of PV1 from 0 PFU to 10^5 PFU and the infection was allowed to proceed for 18hrs. After 18hr post infection (P.I.) cells were detached from the monolayer using trypsin and incubated with 1μM Tat-modified, nuclease-resistant MBs for 30 min. Flow cytomtery

and fluorescent microscope analysis were performed similar to the previous experiment. Prolonging the time allowed the cell-to-cell spread of the infectious virus thus amplifying the signal for detection. As expected, there was a dose dependent increase in the number of fluorescent cells measured (Figure 2.6.). Fluorescent signals were observed from cells that were infected with 1 PFU of PV1 using both the FC assay and fluorescence microscope (Figure 2.7.). These results demonstrate the potential of the MB-FC based method for the direct detection of infective viruses within at very low dosages. It should be noted that the 18hrs time frame is still shorter when compared to a 48 hr incubation period for a traditional plaque assay.

Rapid detection of PV1 infected cells

Rapid detection of viral infection is crucial since the efficacy of most drugs is the highest when administered within 48 hours of infection. Since we have demonstrated the ability of this method to detect even very few infected cells, it was important to determine the time scale of detection in order to be used as a rapid diagnostic test. We performed an experiment where BGMK cells were infected with a low infectious dose (10 PFU) of PV1 for 18hrs. The infected cell suspension was mixed with 1μM Tat-modified, nuclease resistant MBs and immediately monitored in real time using a fluorescence microscope. Fluorescent images using the GFP channel were acquired every 5 seconds for up to 30 min in a fixed area of exposure. Figure 2.8. shows an increase in the number of fluorescent cells at 6 different time points. It was observed that several cells exhibiting dim fluorescence began to appear as early as 30 sec and the intensity of fluorescence

within the cells increased over a period of time. This indicates that with time there were more beacons that internalized and hybridized to the target viral RNA causing an amplified fluorescent signal. Also, there was an increase in the number of fluorescent cells from 0 to 30 min with the fluorescence finally saturating at 30 min. This could suggest that the highly infected cells that have an abundance of the target viral RNA can fluoresce immediately upon MB uptake; the slight time delay observed in some cells may be a result of the different stages of infection or the slightly difference time scale in MB uptake.

In conclusion, the MB flow based system is a simple, rapid and sensitive approach to monitor viral infection and detect the presence of virus infected cells, thereby making it a potential diagnostic tool.

References

1. Robertson, K., A. B. Verhoeven, D. C. Thach, and E. L. Chang. 2010. Monitoring viral RNA in infected cells with LNA flow-FISH. *RNA*. 16:2-7.

2. Rabenau, H. F., H. H. Kessler, M. Kortenbusch, A. Steinhorst, R. B. Raggamb, and A. Berger. 2007. Verification and validation of diagnostic laboratory tests in clinical virology. *J. Clin. Virol.* 40:93-98.

3. Mahy, B. W. J., and H. O. Kangro. 1996. *Virology methods manual*. Academic press, 3-144.

4. Drake, T. J., and W. Tan. 2004. Molecular beacon DNA probes and their bioanalytical applications. *Appl. Spectrosc*. 58:269-280.

5. Fang, X., J. J. Li, J. Perlette, W. Tan, and K. Wang. 2000. Molecular beacons: novel fluorescent probes. *Anal. Chem*. 72:747A-753A.

6. Goel, G., A. Kumar, A. K. Puniya, W. Chen, and K. Singh. 2005. Molecular beacon: a multitask probe. *J. Appl. Microbiol*. 99:435-442.

7. Santangelo, P. J. 2010. Molecular beacons and related probes for intracellular RNA imaging. *Nanomedicine and Nanobiotechnology*. 2:11-19.

8. Sokol D. L., X. Zhang, P. Lu, and A. M. Gerwirtz. 1998. Real time detection of DNA-RNA hybridization in living cells. *Proc. Natl. Acad. Sci. U. S. A*. 95:11538–11543.

9. Tyagi, S., and F. R. Kramer. 1996. Molecular beacons: probes that fluoresce upon hybridization. *Nat. Biotechnol*. 14:303-308.

10. Marras, S. A. E., F. R. Kramer, and S. Tyagi. 1999. Multiplex detection of single-nucleotide variations using molecular beacons. *Genet. Anal-Biomol. E.* 14:151-156.

11. Tyagi, S., D. P. Bratu, and F. R. Kramer. 1997. Multicolor molecular beacons for allele discrimination. *Nat. Biotechnol.* 16:49-53.

12. Tyagi, S. and O. Alsmadi. 2004. Imaging native β-actin mRNA in motile fibroblasts. *Biophys.* 87:4153-4162.

13. Yeh, H.-Y., Y. C. Hwang, M. V. Yates, A. Mulchandani, and W. Chen. 2008. Detection of hepatitis A virus using a combined cell culture-moleuclar beacon assay. *Appl. Environ. Microbiol.* 74:2239-2243.

14. Yeh, H.-Y., M. V. Yates, A. Mulchandani, and W. Chen. 2008. Visualizing the dynamics of viral replication in living cells via Tat peptide delivery of nuclease-resistant molecular beacons. *Proc. Natl. Acad. Sci. U.S.A.* 105:17522-17525.

15. Bordignon, J., S. C. Pires Ferreira, G. M. Medeiros Caporale, M. L. Carrieri, I. Kotait, H. C. Lima, and C. R. Zanetti. 2002. Flow cytometry assay for intracellular rabies virus detection. *J. Virol. Methods.* 105:181-186.

16. Lambeth, C. R., L. J. White, R. E. Johnston, and A. M. de Silva. 2005. Flow cytometry- based assay for titrating dengue virus. *J. Clin. Microbiol.* 43:3267-3272.

17. Defoort, J.-P., M. Martin, B. Casano, S. Prato, C. Camilla, and V. Fert. 2000. Simultaneous detection of multiplex-amplified human immunodeficiency virus type 1 RNA, hepatitis C virus RNA, and hepatitis B virus DNA using flow

cytometer microsphere based hybridization assay. *J. Clin. Microbiol.* 38:1066-1071.

18. Kao, C. L., M. C. Wu, Y. H. Chiu, J. L. Lin, Y. C. Wu, Y. Y. Yueh, L. K. Chen, M. F. Shaio, and C. C. King. 2001. Flow cytometry compared with indirect immunofluorescence for rapid detection of dengue virus type 1 after amplification in tissue culture. *J. Clin. Microbiol.* 39:3672-3677.

19. Cantera, J. L., W. Chen, and M. V. Yates. 2010. Detection of infective Poliovirus by a simple, rapid, and sensitive flow cytometry method based on fluorescence resonance energy transfer technology. *Appl. Environ. Microbiol.* 76:584-588.

20. De La Torre, J. C., E. Wimmer, and J. J. Holland. 1990. Very high frequency of reversion to guanidine resistance in clonal pools of guanidine-dependent type 1 poliovirus. *J. Virol.* 64:664-671.

Legends to Figures

Fig. 2.1. Schematic representation of the principle and design of a molecular beacon. The molecular beacons (MBs) form a closed hairpin structure in the absence of a complementary target. The proximity of the quencher (3') to the fluorophore (5') results in a loss of fluorescence signal. In the presence of a complementary viral RNA target, the MB opens up; this can be directly measured as a fluorescent signal. Hybridization with complementary target RNA results in a direct fluorescent signal.

Fig. 2.2. Quantification of poliovirus 1 (PV1) infection of BGMK cells using flow cytometry. Confluent monolayers of BGMK cells (1.5 X 10^5 cells) in 8 well chamber wells were infected with 10^5 PFU of PV1 for 18hrs. After 18hr post infection (P.I.) cells were detached from the monolayer using trypsin and prepared by mixing populations of highly infected cells with uninfected cells to represent different percentages of infection (0%, 1%, 2%, 5%, 10%, 20% and 100%) . The cells were washed with 10% FBS followed by 1X TBS with 3mM EDTA (pH 8.0); mixed with 1μM MB-PV1 and subjected to flow cytometry. In the histogram the x axis is the GFP intensity and the y axis represents the number of cells for uninfected sample, infected sample and different percentages of the infection mixture.

Fig. 2.3. The correlation between the percentage of fluorescent cells measured by FC and the percentage of infected cells in the mixture. Cells were infected with PV1; harvested and incubated with 1μM MB-PV1as described previously. The percentage of infected

cells shown in the graph was determined by counting the number of fluorescent cells and dividing it by the total number of cells counted.

Fig. 2.4. Visualization of BGMK cells infected with different percentages of PV1 infection. Cells were infected with PV1 for 18 hrs; harvested and incubated with 1μM MB-PV1as described previously. Fluorescent images (GFP channel) and DIC images were acquired and merged to provide a composite image.

Fig. 2.5. Direct comparison of FC assay and fluorescence microscope assay. Varying percentages of PV1 infected cells (0%, 1%, 2%, 5%, 10%, 20% and 100%) incubated with 1μM MB-PV1were prepared and analyzed using flow cytometry and fluorescence microscope. The fluorescent and DIC images from 5 different fields within the chamber well were captured using a 20X magnification and the percentage of fluorescent cells was recorded and averaged.
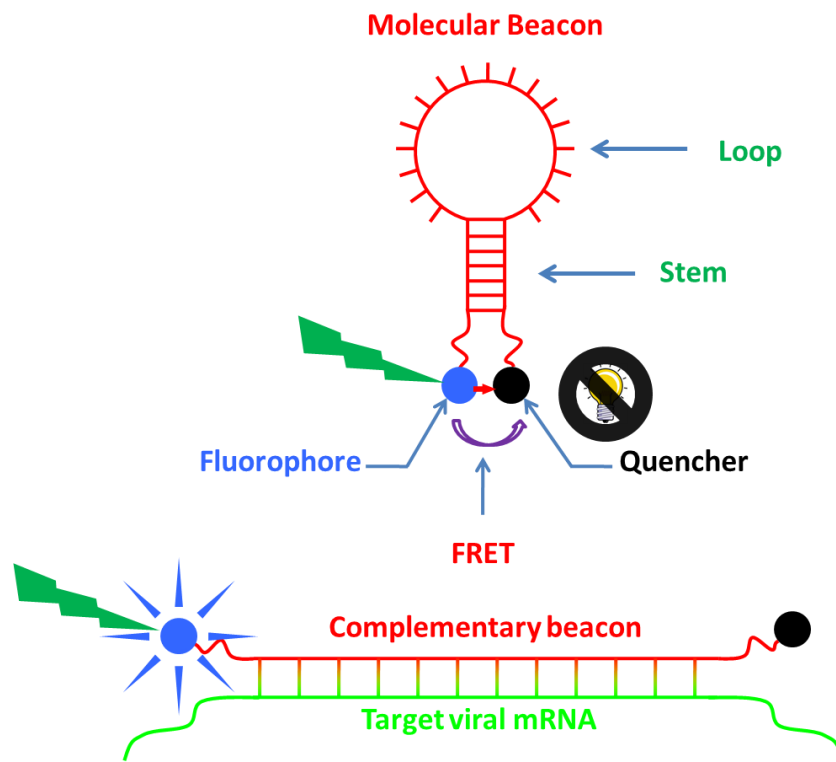
Fig. 2.6. Quantification of PV1 infectious virus dosage using flow cytometry. Confluent monolayers of BGMK cells were infected with varying dose of PV1 from 0 PFU to 10^5 PFU for 18hrs. After 18hr post infection (P.I.) cells were detached from the monolayer mixed with 1μM MB-PV1 and subjected to flow cytometry. The percentage of infected cells shown in the graph was determined by counting the number of fluorescent cells and dividing it by the total number of cells counted.

Fig. 2.7. Visualization of BGMK cells infected with varying dose of PV1 infection. Cells were infected with PV1 for 18hr; harvested and incubated with 1μM MB-PV1as
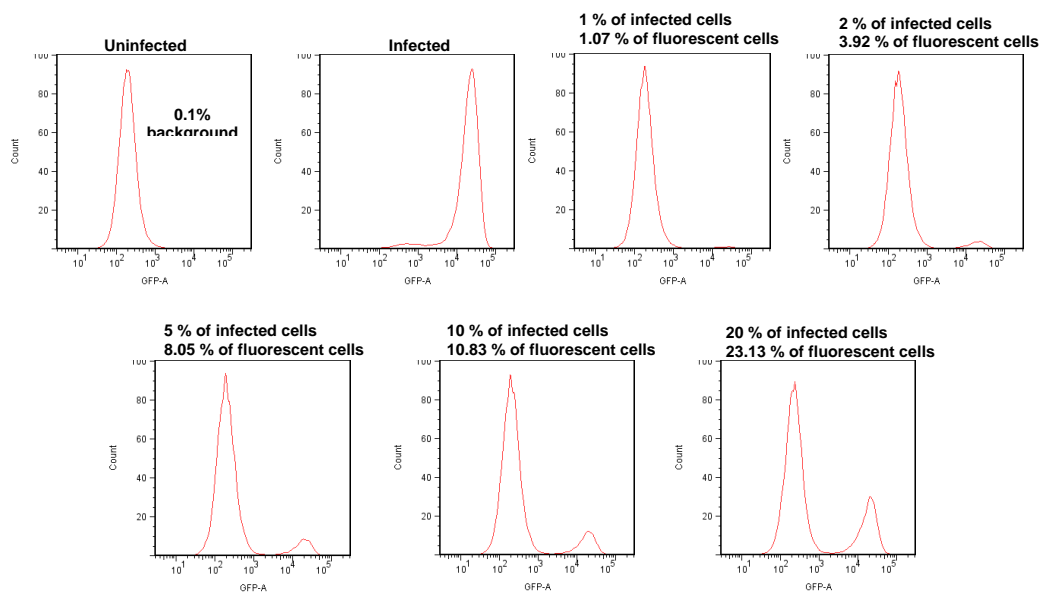
described previously. Fluorescent images (GFP channel) and DIC images were acquired and merged to provide a composite image.

Fig. 2.8. Real time detection of PV1 in BGMK cells. Cells were infected with 10 PFU PV1 for 18hrs; detached and incubated with 1μM MB-PV1and monitored in real time using a fluorescence microscope from 0 to 30min.
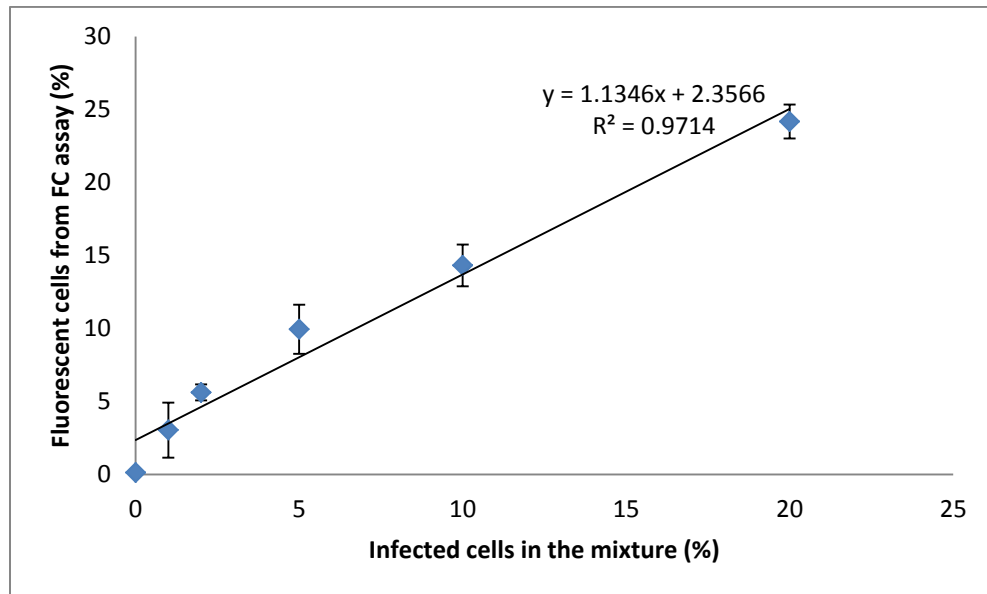
Fig. 2.1.

Fig. 2.2.

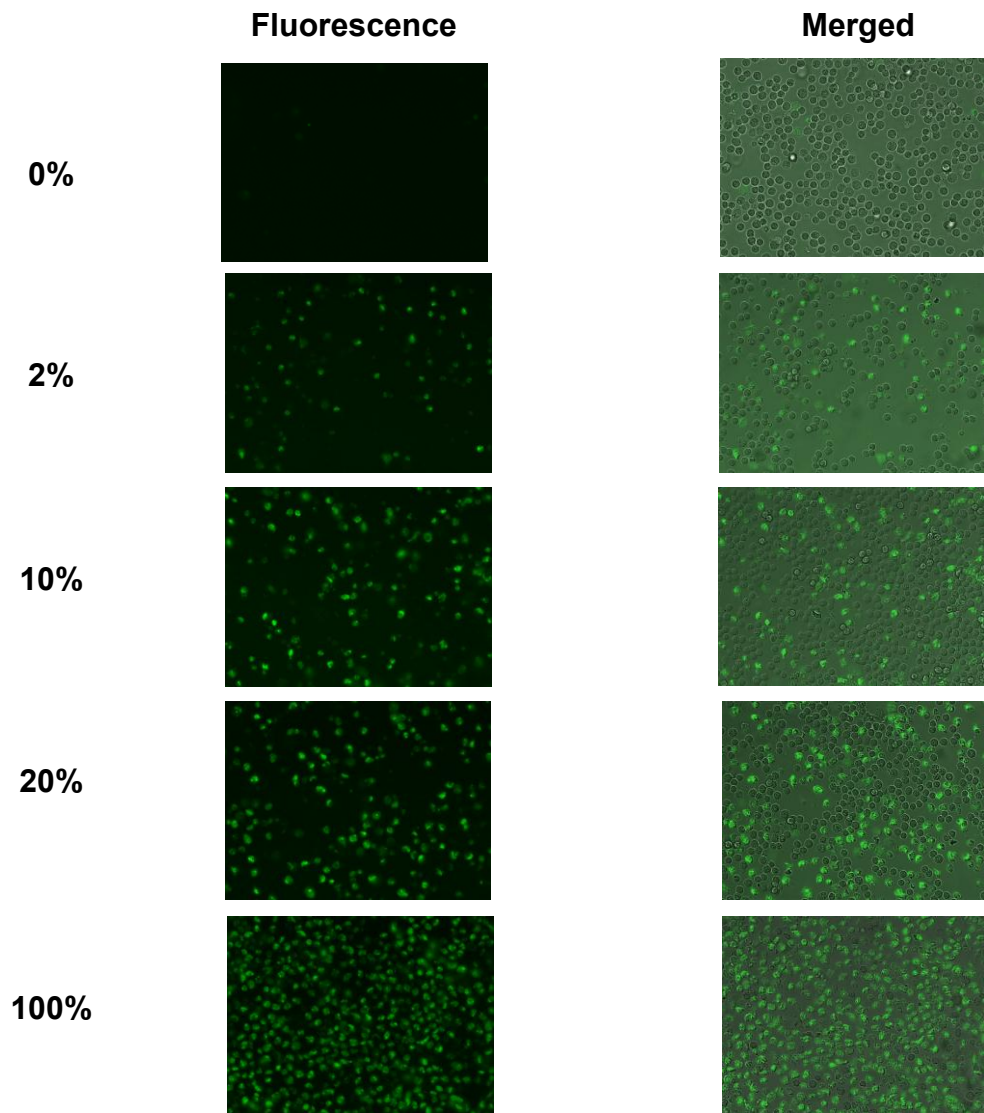**Fig. 2.3.**

Fig. 2.4.

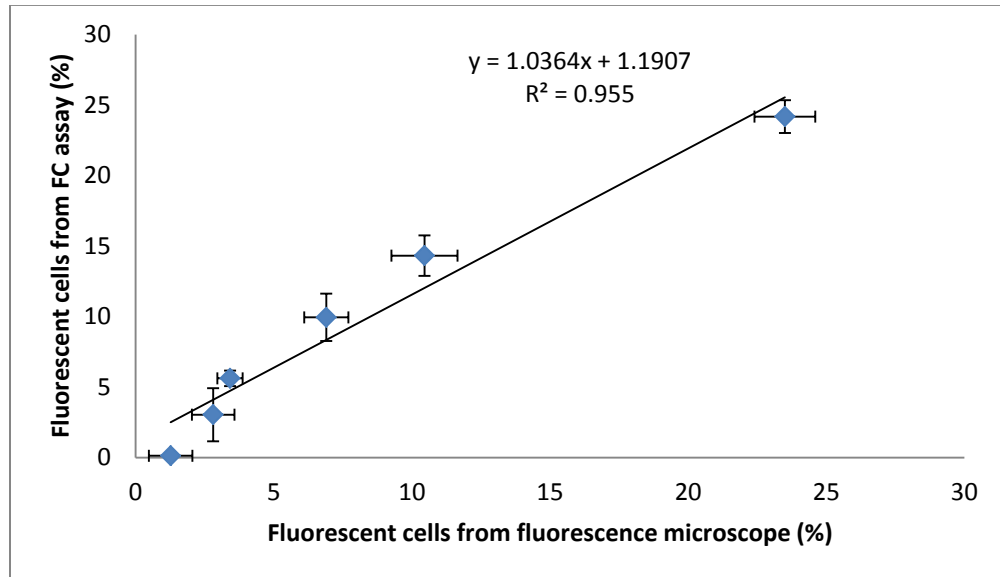|	Fluorescence	Merged
0%		
2%		
10%		
20%		
100%		

Fig. 2.5.

Fig. 2.6.

Fig. 2.7.

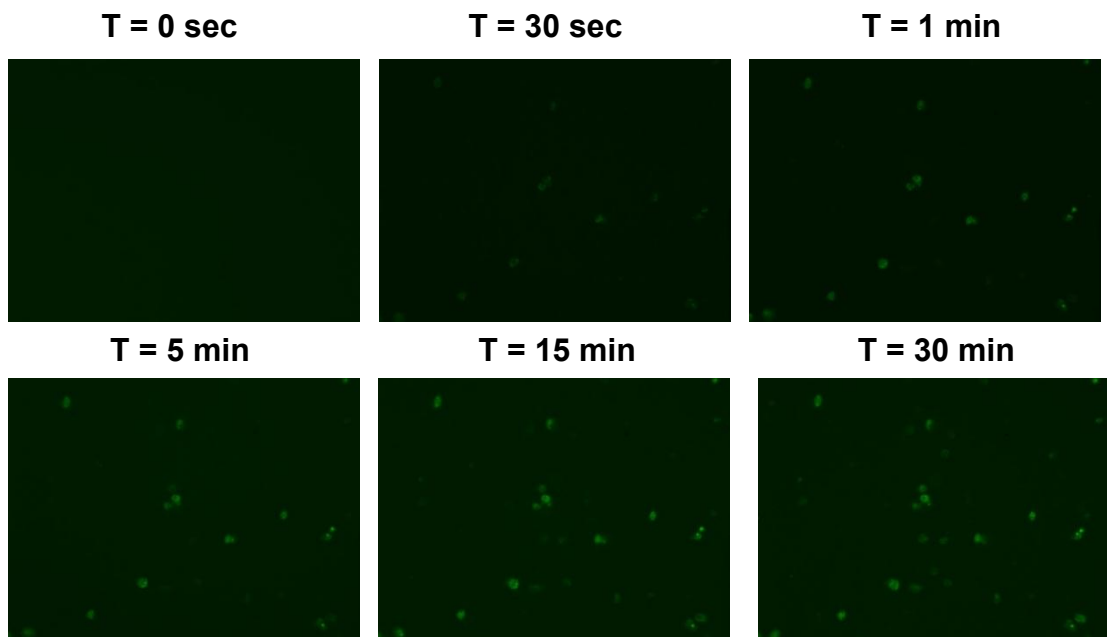|	Fluorescence	Merged
0 PFU		
1 PFU		
100 PFU		
10000 PFU		

Fig. 2.8.

T = 0 sec   T = 30 sec   T = 1 min

T = 5 min   T = 15 min   T = 30 min
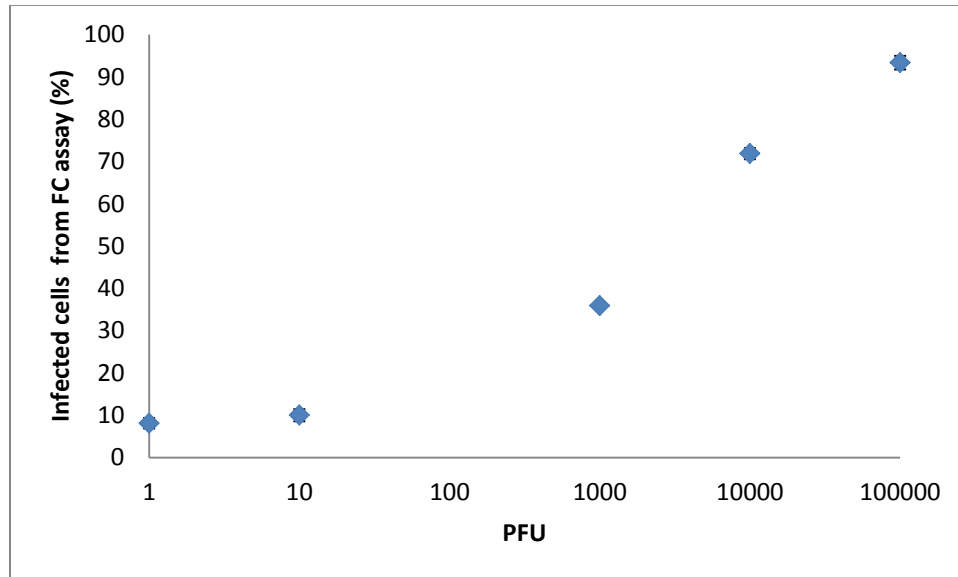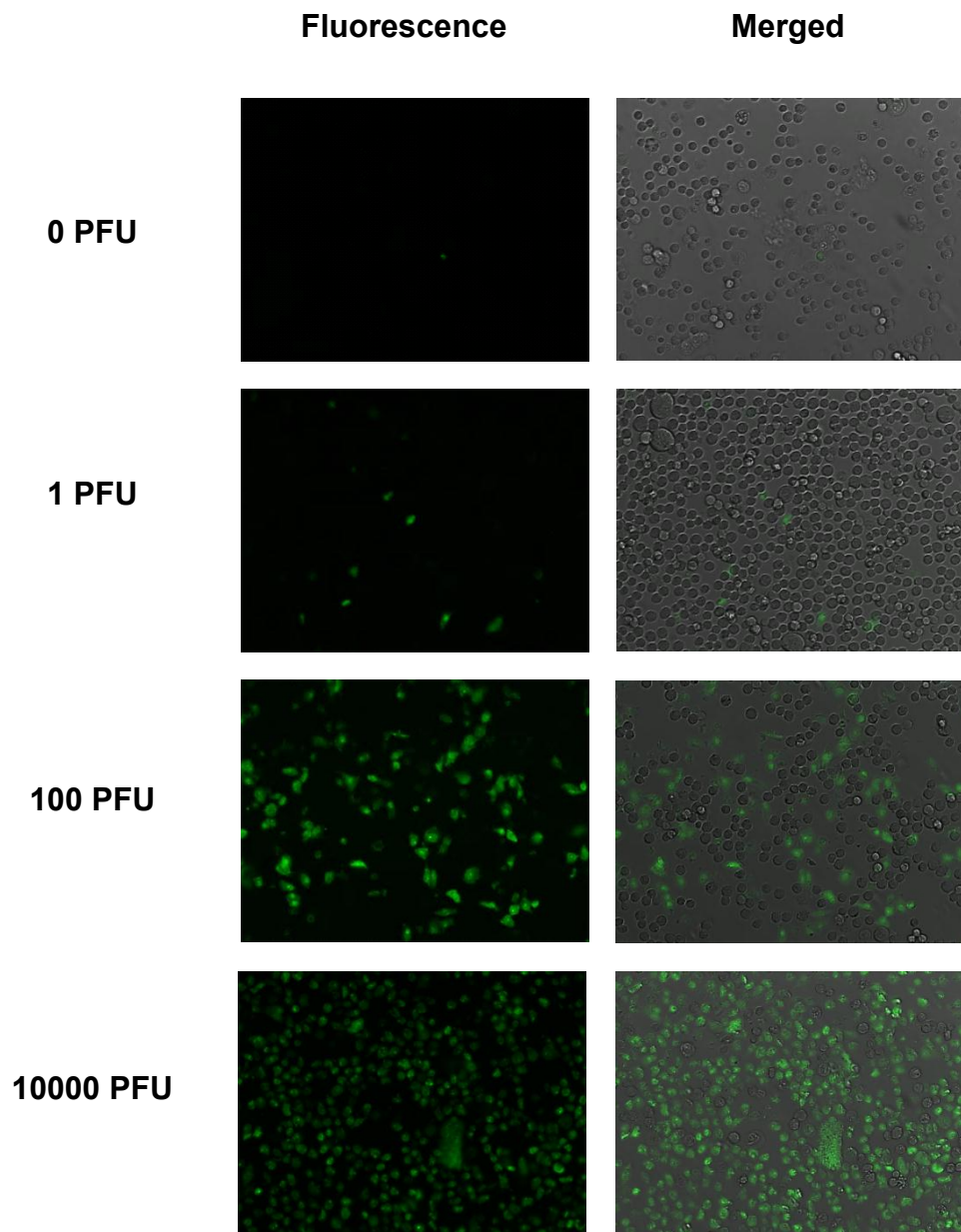
Chapter 3

Detection of Influenza A virus in living cells using molecular beacons

Abstract

Diagnostics plays a vital role in the detection of epidemiologically important viruses and identification of appropriate treatments. Influenza is one of the most important infectious diseases of humans due to the emergence of novel strains during every flu season. The reassortment of genes between two (or more) influenza viruses of the same or different subtype leads to the formation of genetically novel viruses. Since the efficacy of most drugs is the highest when administered within 48 hours of infection, rapid diagnosis is crucial to successful treatment. Traditionally immunological, nucleic acid-based and infectivity-based methods have been used to perform virus analysis, but these methods can take up to weeks to enable detection. Molecular beacons (MBs) are one among the promising technologies that are used for gene detection in living cells. MBs are single-stranded oligonucleotide probes that possess a stem-loop structure consisting of a fluorophore at one end and a quencher at the other. The probes are specific for a target nucleotide sequence and produce fluorescence upon target binding. To preserve the duplex stability of MB in living cells, they have been modified with a 2'-O-methyl substitution and phosphorothioate internucleotide linkages to avoid endogenous nuclease degradation. A non-invasive strategy for intracellular delivery of the MBs was used which consists of the HIV-1-derived Tat peptide. This Tat-based method coupled with nuclease-resistant MBs can provide powerful means for rapid detection and a potential diagnostic tool that can even distinguish between subtypes of viruses with high specificity and sensitivity.

Introduction

Influenza is one of the most important infectious diseases of humans. The annual mortality that is caused by influenza in the United States alone is estimated at over 36,000 (1) whereas occasional global pandemics can infect 20–40% of the world population in a single year. Influenza viruses are enveloped, single-stranded, negative sense RNA viruses that belong to the family Orthomyxoviridae. They are responsible for regular seasonal epidemics in humans, other mammalian species and birds (2). Currently, three distinct types of influenza virus (A, B and C) are circulating globally in human populations, although type A viruses exhibit the greatest genetic diversity and infect the widest range of host species (3). The genome of influenza A virus is composed of eight segments that can be exchanged through reassortment. Influenza A viruses can be classified into subtypes based on two surface glycoproteins: hemagglutinin (HA) and neuraminidase (NA). At this time, 16 distinct haemagglutinins and 9 neuraminidases have been identified (4). Adaptation of pathogenic avian viruses to humans can occur either by mutation or reassortment, leading to potentially very serious pandemics (5-6). Due to this ability to cross the species barrier, influenza A viruses are a permanent threat to human health and rapid diagnosis of the virus is crucial. Appropriate treatment of patients with respiratory illness depends on accurate and timely diagnosis of the influenza A subtype circulating during a regular flu season.

The current diagnostic tests available for detecting influenza virus conducted by laboratories include viral culture, polymerase chain reaction (PCR), rapid antigen testing,

and immunofluorescence (7). There are also commercial rapid diagnostic tests available that are being used by laboratories to detect influenza viruses within 30 minutes (8-9). However, some of these tests don't provide any information about influenza A subtypes and exhibit low sensitivity (10). Immunofluorescence (fluorescent antibody staining) is another commonly used technique that can generally yield test results in 2 to 4 hours and sensitivities are generally higher than rapid tests, but lower than viral culture (11-12). Direct observation of cytopathic effects (CPE) using cell culture is still being used, but often does not provide results in time to help with clinical decisions such as the use of antiviral drug treatment. Reverse-transcriptase polymerase chain reaction (RT-PCR) testing for influenza viruses is available at a limited number of laboratories, but the samples are subject to bacterial contamination (13). To address some of the drawbacks of the above mentioned methods, there is a need for an improved method capable of rapid, accurate identification and subtyping of influenza viruses.

Among the various methods reported till date, molecular beacons (MBs) are considered one of the most promising technologies currently under development for real-time gene detection. MBs are single stranded, oligonucleotide probes with a hair pin structure that fluoresce upon hybridizing to a complementary target sequence via fluorescence resonance energy transfer (FRET) (14-15). The spontaneous hybridization that occurs between the beacon and the target is highly specific and can be used to differentiate even a single base pair mismatch (16-17). This ability of the beacon to recognize even a single nucleotide mismatch is highly promising to differentiate between subtypes of viruses that possess fairly conserved genomes. MBs have been widely used

in many areas, such as in real-time monitoring of DNA/RNA amplification during PCR, gene typing, mutation detection, real-time enzymatic cleavage assay and RNA detection in living cells (18-21), however, their applications for viral detection in infected cells have been reported only recently (22-23). The use of nuclease-resistant, MBs for real-time detection of coxsackievirus replication in living cells via Tat peptide delivery has been successfully demonstrated in a recent report (24). One can easily envision an adaptation of this technique as a diagnostic tool to detect the presence of influenza A virus infected cells. We imagine that a better understanding of the dynamic behavior of viral replication could be gained through *in vivo* experiments and could extend to therapeutic studies of disease pathophysiology, drug discovery, and antiviral treatments.

Materials and Methods

MDCK Cell Culture

Mardin Darby Canine Kidney (MDCK) (ATCC# CCL-34) cells are the preferred cell line for the isolation and characterization of influenza viruses. MDCK cells were cultured in Eagle's minimal essential medium (EMEM) (ATCC # 30-2003) supplemented with 10% fetal bovine serum (FBS; Hyclone) and 100U/ml of penicillin and 100µg/ml of streptomycin (Hyclone).   Cells were grown in an incubator maintained at 37°C and 5% (vol/vol) CO_2. Phosphate-buffered saline solution (PBS; 0.01M phosphate, pH 7.4, 0.138 M Na Cl, and 2.7mM KCl) and Tris-buffered saline solution (TBSS; 0.05M Tris, pH 7.4, 0.28 M NaCl, 10mM KCl, and 0.82mM Na_2HPO_4) were used during the washing steps for MDCK cell culture.

Influenza Virus preparation

Influenza A virus (H1N1) strain A/PR/8/34 (ATCC # VR-95) and influenza A (H3N2) strain Hong Kong/8/68 (ATCC # VR-544) was propagated in MDCK cells for upto 5 days at 37°C.The cells were monitored daily to observe the cytopathic effect (CPE) on the monolayer. The cell culture supernatant was harvested when 75% of the cells were exhibiting CPE. The virus stock was harvested for 15min at 300 x g at 4 C to pellet the cell debris. The fresh virus stock was stored as 500µl aliquots at -80°C until use.

Quantification of Influenza virus by plaque assay

The influenza virus stock was thawed in cool water and stored at 4°C to reduce the loss of infectivity. A 10-fold series dilution of the virus stock was prepared in the plaque assay wash medium that consists of Dulbecco's modified eagle's medium (DMEM) (ATCC # 30-2002) supplemented with 100U/ml penicillin and 100µg/ml streptomycin (Hyclone). MCDK cells were grown to 90% confluency in 6-well plates (Costar; Corning) and washed thrice using plaque assay wash medium to remove any remaining fetal bovine serum (FBS) present in the solution. FBS inhibits the entry of the virus and hence must be removed for efficient infection of cells. MDCK cells were then inoculated with 100µl of diluted virus sample and incubated for 1hr at 37°C. After 60min of adsorption, the wells were washed twice using plaque assay wash medium. The solutions were aspirated and an equal mixture of 1.6% agarose and 2X plaque assay medium containing 2X DMEM supplemented with 200U/ml penicillin and 200µg/ml streptomycin, 4mM L-glutamine, 50mM HEPES buffer (pH 7.4), 2mg/ml of TPCK-trypsin (Sigma-Aldrich) was added to each well. The solution was allowed to solidify at room temperature before incubating at 37°C incubator. After 72 hrs of incubation, the agar plug was carefully removed from each well using sterile forceps. The cells were then fixed by adding 2ml of 70% ethanol to each well and incubating at room temperature for 20 min. The ethanol was aspirated and cells were stained with 0.8% crystal violet solution for 10 min. The excess stain was removed by washing with de-ionized water and virus plaques were counted to calculate the titre of the stock (Figure 3.1.).

Molecular beacon design

The probe was designed based on genome sequence and structure of Influenza A virus [A/Puerto Rico/8/34(H1N1)] using GenBank database and NCBI BLAST. To study the thermodynamic properties and predict secondary structures of the MB, a DNA folding program *mfold* (www.bioinfo.rpi.edu) was used. The molecular beacon (MB-N1) (5'-6FAM- CCgAC**TTTCAgTTATTATgCCgTTgTATTT**gTC/thiol-dG/gg – BBQ- 3') was designed to be perfectly complementary to the nucleotides in 574-598 (NC_002018 NCBI database) region of the neuraminidase (NA) segment of influenza A virus (H1N1) genome. The beacon was synthesized possessing a 2'-O-methylribonucleotide backbone with phosphorothioate internucleotide linkages by TIB Molbiol. The thiol group near the 3' end of the beacon is for conjugation with a maleimide group attached to the C terminus of the Tat peptide to form a thiol-maleimide linkage. The MB-N1 was solubilized in 100mM Tris-HCl (pH 8.0) buffer containing 1mM $MgCl_2$ to make a stock concentration of 100μM and stored at -20°C as 50μl aliquots until use.

Peptide Design

The C terminal maleimide modified Tat peptide Tyr-Gly-Arg-Lys-Lys-Arg-Arg-Gln-Arg-Arg-Arg-N-CH_2CH_2-N-maleimide (Global Peptide) was mixed with MB-N1 in the molar ratio of 1:1.5. The reaction was allowed to occur at room temperature in the dark for 2 h to form a stable thiol-maleimide bond. The Tat peptide-conjugated with MB-N1 (MB-N1-Tat) was aliquoted and stored at -20°C for experimental use.

Infection of MDCK with Influenza A virus

MDCK cells were grown in 8 well Lab-Tek Chamber slide (Thermo Scientific- NUNC) at 37°C in 5% CO_2 (vol/vol) until 90% confluent. After aspirating the incubation medium, the cell monolayer was washed twice with 1 X phosphate buffered saline solution (PBS) and incubated with different dilutions of H1N1 or H3N2 virus in influenza A virus growth medium containing EMEM supplemented with 7.5% bovine serum albumin (BSA) (Hyclone) and 2µg/ml TPCK-trypsin stock. The virus was allowed to adsorb to the cell surface for 60min at 37°C then the unbound virus particles were removed. The cells were then resealed with influenza A virus growth medium and infection was allowed to proceed.

Delivery of Tat conjugated MB's into infected cells

After different post infection (P.I.) time points, the incubation media in the virus infected MDCK was aspirated. Both control (uninfected) and infected cells were washed twice with 1X PBS buffer and replaced with 1 X Leibovitz L-15 medium (Invitrogen). The Leibovitz L-15 medium contains no phenol red and is a CO_2 independent media making it suitable to perform real time experiments using the fluorescence microscope. MB-N1 (2µM) was slowly added to the infected cells and incubated at 37°C in the dark for 30 min prior to imaging.

Fluorescence microscopy and image processing

A Zeiss Axiovert 40 CFL inverted microscope supplied with an HBO 50W/AC mercury lamp (for fluorescence) and a12-V, 35-W halogen lamp was used to perform live cell imaging. For each sample well, both phase contrast and fluorescent pictures were taken. Image acquisition and processing was carried out using the Image-Pro analysis software (Media Cybernetics). All settings for image capture were kept consistent and the exposure time for each sample was maintained throughout the course of the experiment.

Enumeration of fluorescent cells

To calculate the number of infected cells, firstly multiple phase contrast images of each well were taken to count the total number of cells. Simultaneously, the number of fluorescent cells was counted within those frames using Image-Pro PLUS analysis software.

Results and Discussion

Visualizing influenza A virus mRNA in living MDCK cells

A better understanding of the replication process and the kinetics of influenza A virus infection is necessary to arrive at a suitable diagnostic technique. To visualize viral mRNA in living cells, MB-N1 was delivered into influenza virus-infected MDCK cells by TAT-peptide mediated delivery at various time points post infection (P.I.). MDCK cells were infected with a multiplicity of infection (M.O.I.) of 0.1 PFU/cell. At various P.I. time points starting with 2 hrs, the MDCK cells were incubated with 1μM MB-N1 and the beacons were allowed to internalize for 30 min prior to imaging. At 2.5 h P.I., the resulting fluorescence signals were observed under a fluorescence microscope using a GFP channel (475nm/520nm).The same procedure was repeated for 4, 6, 8, 12, and 18 hr P.I. time points. As early as 2.5hr P.I. a weak fluorescence signal was observed from a few infected cells and at 4 hr P.I., a much brighter fluorescent signal was observed in the cytoplasm of influenza infected MDCK cells; uninfected cells that were also incubated with MB-N1 showed little or no fluorescence (Figure 3.2.). This result ensured that the fluorescent signals in the cytoplasm of influenza virus-infected cells came only from the hybridization of mRNA with MBs, and were not caused by the degradation of MBs. Although the number of fluorescent cells increased from 2.5 hr P.I. to 4 hr P.I., a steady decrease in both fluorescence intensity and number of fluorescent cells was observed thereafter (Figure 3.3.). This could be attributed to the kinetics of mRNA synthesis and mRNA export (25). It has been reported previously that the average life-cycle of the

influenza virus was estimated to be ~11hr (26) and the half- life of a free infectious particle is ~3hrs indicating that the decrease in fluorescent signal that was observed after 4 hr P.I., was a result of the viral mRNA being packaged into new virions and therefore unavailable for the beacon to hybridize. This is consistent with subsequent increase in the fluorescence intensity after 12 hr P.I., suggesting the initiation of a second round infection and the further cell-to-cell spread of the virus. Because of the second round of infection, there is an increase in the number of viral mRNA available for binding which is directly translated to an amplified fluorescence signal at 18 hr P.I. Thus, the results obtained from this experiment correlate directly with reports in literature thereby validating the ability of MB-N1 to accurately capture the infection process of influenza A virus in MDCK cells.

Influenza A virus (H1N1) dosage analysis using MB-N1

In order to develop this method as a diagnostic test, it is imperative to detect very low infectious dosages of the virus. To determine if the system could detect as few as 1 PFU, MDCK cells were infected with varying dosage of H1N1 from 0 PFU to 10^5 PFU and the infection was allowed to proceed for 18hrs. After 18hr post infection (P.I.), cells were detached from the monolayer using trypsin and incubated with 1µM Tat-modified, nuclease-resistant MB-N1 for 30 min. Fluorescence microscopy was performed similar to the previous experiment. Prolonging the time allowed the cell-to-cell spread of the infectious virus thus amplifying the signal for detection. As expected, there was a dose dependent increase in the number of fluorescent cells measured (Figure 3.4.). As early as

18 hr P.I., fluorescent signals was observed from cells that were infected with 1 PFU of H1N1 using fluorescence microscope. These results demonstrate the ability of the MB-N1 to detect very few infected cells which will be crucial in analyzing clinical samples collected from patients at early stages of the disease.

Testing the Specificity of MB-N1 with Influenza A virus (H3N2) infection

One of the most attractive properties of the MBs is their ability to detect and bind to targets with high specificity enabling them to distinguish targets from one another by as little as a single nucleotide. To test the capability of this method to differentiate between different subtypes of influenza A virus, an experiment was performed by infecting MDCK cells with influenza A virus H3N2 at an M.O.I. of 0.1. Similarly, cells were also infected with influenza A virus H1N1 to be used as a positive control. The infection was allowed to proceed for 18 hrs. After 18hr P.I., cells were detached from the monolayer using trypsin and incubated with 1µM Tat-modified, nuclease-resistant MB-N1 for 30 min. Fluorescence microscope analysis was performed similar to the previous experiment. As seen in Figure 3.5., a large number of fluorescent cells were observed in the cytoplasm of H1N1-infected MDCK cells, while uninfected cells that were also incubated with MB-N1 showed little or no fluorescence. As expected, virtually no fluorescent cell was detected in MDCK cells infected with the H3N2 subtype, consistent with the specific nature of MB. The fluorescent signal obtained from the GFP channel was measured for all the samples (uninfected, infected with H1N1 and infected with

H3N2) and analysis was performed using Image-pro- PLUS software. The relative fluorescence intensity was calculated by normalizing the fluorescence intensity values from each of the samples with intensity from uninfected cells. Figure 3.6. shows a plot of the relative fluorescence intensity measured for uninfected, H1N1 infected and H3N2 infected MDCK cells. It was evident from the graph that the signal obtained from H1N1 infected cells using MB-N1 was three times higher when compared to the uninfected cells (negative control). Also, the signal from H3N2 infected cells was only virtually identical to the control. This further validates the application of our technique to successfully differentiate between subtypes of influenza A virus.

Rapid detection of H1N1 infected cells

Rapid diagnosis of an infectious disease is crucial since the efficacy of most drugs is the highest when administered within 48 hours. Since we have demonstrated the ability of this method to detect even few infected cells, in order to be used as a rapid diagnostic tool it was important to determine the time scale of detection. We performed an experiment where MDCK cells were infected with an M.O.I of 0.1 PFU/cell of H1N1 and the infection was allowed to proceed for 18hrs. After 18hr post infection (P.I.), samples were trypsinized and collected in a suspension form. The infected cell suspension was mixed with 1μM Tat-modified, nuclease resistant MBs and immediately monitored using a fluorescence microscope. Fluorescent images using the GFP channel was acquired every 5 seconds for up to 30 min in a fixed area of exposure. Figure 3.7. shows an increase in the number of fluorescent cells at 6 different time points. It was observed that several

cells exhibiting dim fluorescence began to appear as early as 30 sec and the intensity of fluorescence increases over a period of time suggesting that with time there are more beacons that internalize and bind to the target viral RNA. Also, there was an increase in the number of fluorescent cells from 0 to 30 min with the fluorescence finally saturating at 30 min. This time line of detection reported here is similar to the current rapid diagnostic tests that are commercially available and is used by laboratories to detect influenza viruses within 30 minutes.

In conclusion, MB-N1 have been successfully used to better understand the dynamic behavior of influenza A viral replication while providing rapid, sensitive, identification and subtyping of the virus.

References

1. Thompson, W. W., D. K. Shay, E. Weintraub, L. Brammer, N. Cox, L. J. Anderson, and K. Fukuda. 2003. Mortality associated with influenza and respiratory syncytial virus in the United States. *JAMA*. 289:179–186.

2. Webster, R. G., W. J. Bean, O. T. Gorman, T. M. Chambers, and Y. Kawaoka. 1992. Evolution and ecology of influenza A viruses. *Microbiol. Rev.* 56:152–179.

3. Nelson, M. I., and E. C. Holmes. 2007. The evolution of epidemic influenza. *Nat. Rev. Genet.* 8:196-205.

4. Samji, T. 2009. Influenza A: Understanding the viral life cycle. *Yale J. Biol. Med.* 4:153-159.

5. Noah, D. L., and R. M. Krug. 2005. Influenza virus virulence and its molecular determinants. *Adv. Virus Res*. 65:121–145.

6. Baigent, S. and J. McCauley. 2003. Influenza type A in humans, mammals and birds: determinants of virus virulence, host-range and interspecies transmission. *BioEssays*. 25:657–671.

7. R. Wang and J. K. Taubenberger. 2010. Methods for molecular surveillance of influenza. *Expert Rev. Anti. Infect. Ther.* 8:517-527.

8. Gavin, P. J., and R. B. Thomson Jr. 2003. Review of Rapid Diagnostic Tests for Influenza. *Clin. and Appl. Imm. Rev.* 4:151-172.

9. Chan, K. H., N. Maldeis, W. Pope, A. Yup, A. Ozinskas, J. Gill, W. H. Seto, K. F. Shortridge, and J. S. M. Peiris. 2002. Evaluation of the Directigen FluA+B Test

for Rapid Diagnosis of Influenza Virus Type A and B Infections. *J. Clin. Microbiol*. 40:1675-1680.

10. Uyeki, T. M., R. Prasad, C. Vukotich, S. Stebbins, C. R. Rinaldo, Y.-H. Ferng, S. S. Morse, E. L. Larson, A. E. Aiello, B. Davis, and A. S. Monto. 2009. Low Sensitivity of Rapid Diagnostic Test for Influenza. *Clin. Infect. Dis.* 48:89-92.

11. A. F. M. S. Rahman. 1973. Early detection of influenza virus in cell culture by means of immunofluorescence. *J. Clin. Pathol.* 26:503-505.

12. Blaskovic, P., and N. A. Labzoffsky. 1973. Immunofluorescence methods for detection of influenza and mumps antibodies using infected shedded allantoic cells and impression smears of organ cultures as the sources of antigens. *Archives of virology.* 41:354-359.

13. Stone, B., J. Burrows, S. Schepetiuk, G. Higgins, A. Hampson, R. Shaw, and T. Kok. 2003. Rapid detection and simultaneous subtype differentiation of influenza A viruses by real time PCR. *J. Virol. Methods*.117:103-112.

14. Marras, S. A. E., F. R. Kramer, and S. Tyagi. 1999. Multiplex detection of single-nucleotide variations using molecular beacons. *Genet. Anal-Biomol E.* 14:151-156.

15. Tyagi, S., and F. R. Kramer. 1996. Molecular beacons: probes that fluoresce upon hybridization. *Nat. Biotechnol*. 14:303-308.

16. Tyagi, S., D. P. Bratu, and F. R. Kramer. 1997. Multicolor molecular beacons for allele discrimination. *Nat. Biotechnol.* 16:49-53.

17. Tyagi, S. and O. Alsmadi. 2004. Imaging native β-actin mRNA in motile fibroblasts. *Biophys*. 87:4153-4162.

18. Fang, X., J. J. Li, J. Perlette, W. Tan and K. Wang. 2000. Molecular beacons: novel fluorescent probes. *Anal Chem*. 72:747A-753A.

19. Goel, G., A. Kumar, A. K. Puniya, W. Chen, and K. Singh. 2005. Molecular beacon: a multitask probe. *J. Appl. Microbiol*. 99:435-442.

20. Galil, K. H. A. E, M. A. E. Sokkary, S. M. Kheira, A. M. Salazar, M. V. Yates, W. Chen and A. Mulchandani. 2004. Combined immunomagnetic separation-molecular beacon-reverse transcription-PCR assay for detection of Hepatitis A virus from environmental samples. *Appl. Environ. Microbiol*. 70:4371-4374.

21. Bratu, D. P*.,* B.-J. Cha, M. M. Mhlanga, F. R. Kramer, and S. Tyagi. 2003. Visualizing the distribution and transport of mRNA in living cells. *Proc. Natl. Acad. Sci. USA*. 100: 13308-13313.

22. Cui, Z. Q., Z. P. Zhang, X. E. Zhang, J. K. Wen, Y. F. Zhou, and W. H. Xie. 2005. Visualizing the dynamic behavior of poliovirus plus-strand RNA in living host cells. *Nucleic Acids Res.* 33:3245-3252.

23. Yeh, H.-Y., Y. C. Hwang, M. V. Yates, A. Mulchandani, and W. Chen. 2008. Detection of hepatitis A virus using a combined cell culture-moleuclar beacon assay. *Appl. Environ. Microbiol*. 74:2239-2243.

24. Yeh, H.-Y., M. V. Yates, A. Mulchandani, and W. Chen. 2008. Visualizing the dynamics of viral replication in living cells via Tat peptide delivery of nuclease-resistant molecular beacons. *Proc. Natl. Acad. Sci. U.S.A*. 105:17522-17525.

25. Wang, W., Z.-Q. Cui, H. Han, Z.-P. Zhang, H.-P. Wei, Y.-F. Zhou, Z. Chen, and X.-E. Zhang. 2008. Imaging and characterizing influenza A virus mRNA transport in living cells. *Nucleic Acids Res.* 36:4913-4928.

26. Baccam, P., C. Beauchemin, C. A. Macken, F. G. Hayden, and A. S. Perelson. 2006. Kinetics of Influenza A Virus Infection in Humans. *J. Virol.* 15:7590-7599.

Legends to Figures

Fig. 3.1. Quantification of influenza A H1N1 virus using plaque assay. A 10-fold series dilution of H1N1 was prepared and MDCK cells were inoculated with 100μl of diluted virus sample and incubated for 1hr at 37°C. The cells were washed and an equal mixture of 1.6% agarose and 2X plaque assay medium. The solution was allowed to solidify at room temperature and incubated at 37°C incubator for 72 hrs. After 3 days of incubation, the agar plug was removed and cells were fixed by adding 2ml of 70% ethanol followed by staining with 0.8% crystal violet. The excess stain was removed and virus plaques were counted to calculate the titre of the stock.

Fig. 3.2. Visualization of influenza A viral mRNA using MB-N1 probes. MDCK cells were infected with influenza A H1N1 at an M.O.I. of 0.1 PFU/cell. At various P.I. time points (2 to 18 hrs) MDCK cells were incubated with 1μM MB-N1 for 30 min prior to imaging. Fluorescent signal from infected cells was visualized under a fluorescence microscope using a GFP channel (475nm/520nm).

Fig. 3.3. Kinetics of influenza infection using MB-N1. MDCK cells were infected with influenza A H1N1 at an M.O.I. of 0.1 PFU/cell. At various P.I. time points (2 to 18 hrs) MDCK cells were incubated with 1μM MB-N1 for 30 min prior to imaging. Fluorescent signal from infected cells was visualized under a fluorescence microscope using a GFP channel (475nm/520nm). Average fluorescence intensity of 4 to 5 different fields was measured using Image-pro-PLUS software.

Fig. 3.4. Quantification of H1N1 infectious virus dosage using MB-N1. Confluent monolayers of MDCK cells were infected with varying dose of H1N1 from 0 PFU to 1000 PFU for 18hrs. After 18hr post infection (P.I.) cells were detached from the monolayer mixed with 1μM MB-N1 and visualized using a fluorescence microscope. Fluorescent images (GFP channel) and DIC images are acquired and merged to provide a composite image.
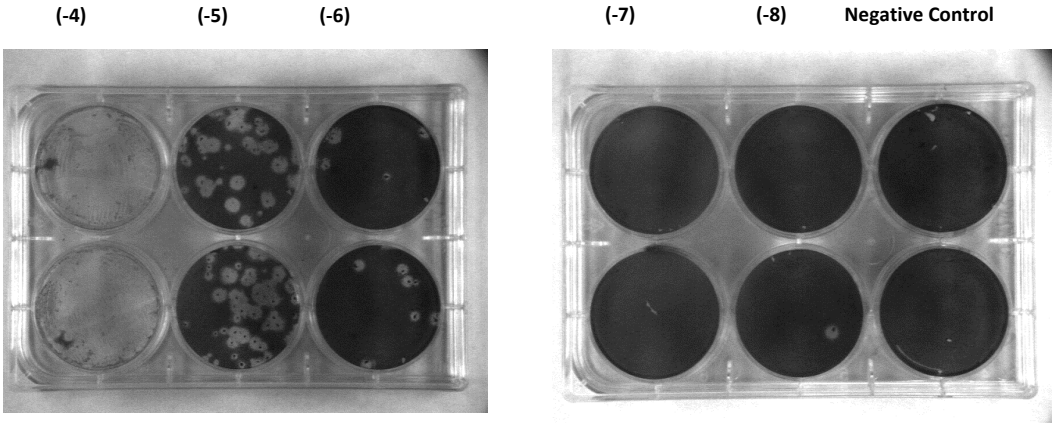
Fig. 3.5. Testing the specificity of MB-N1 with influenza A H3N2 virus. MDCK cells were infected with influenza A virus H3N2 at an M.O.I. of 0.1. Similarly, cells were also infected with influenza A virus H1N1 to be used as a positive control. 18hr P.I., cells were detached from the monolayer using trypsin and incubated with 1μM Tat-modified, nuclease-resistant MB-N1 for 30 min. Fluorescence microscope analysis was performed similar to the previous experiment.

Fig. 3.6. Quantification of relative fluorescence intensity of H1N1 and H3N2 virus infected cells using MB-N1. The fluorescent signal obtained from the GFP channel was measured for all the samples (uninfected, infected with H1N1 and infected with H3N2) and analysis was performed using Image-pro- PLUS software. The relative fluorescence intensity was calculated by normalizing the fluorescence intensity values from each of the samples with intensity from uninfected cells.
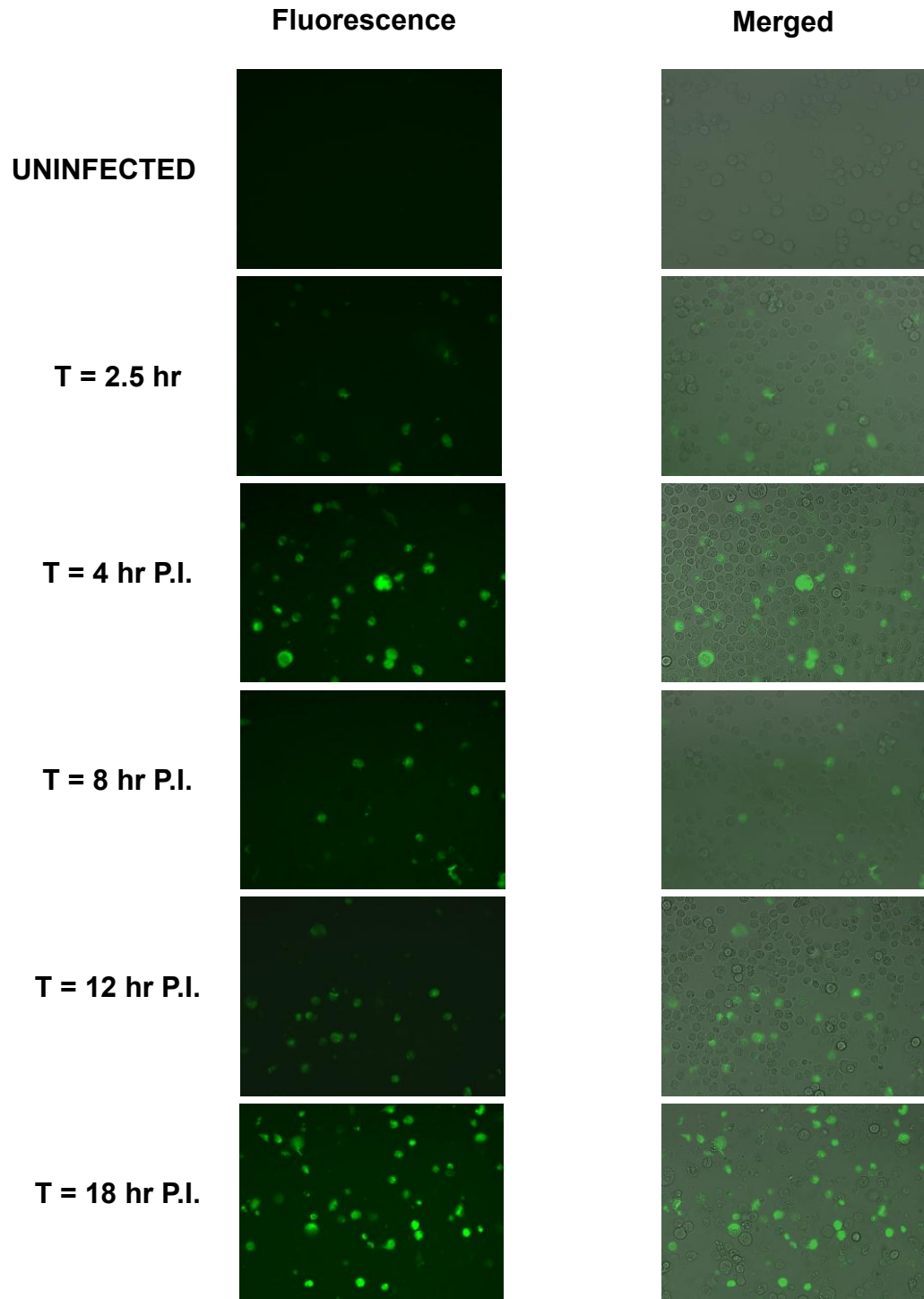
Fig. 3.7. Real time detection of Influenza A H1N1 in MDCK cells. Cells were infected with H1N1 at an M.O.I of 0.1 PFU/cell for 18hrs. 18hr P.I., cells were detached and

incubated with 1μM MB-PV1and monitored in real time using a fluorescence microscope

from time 0 to 30min.

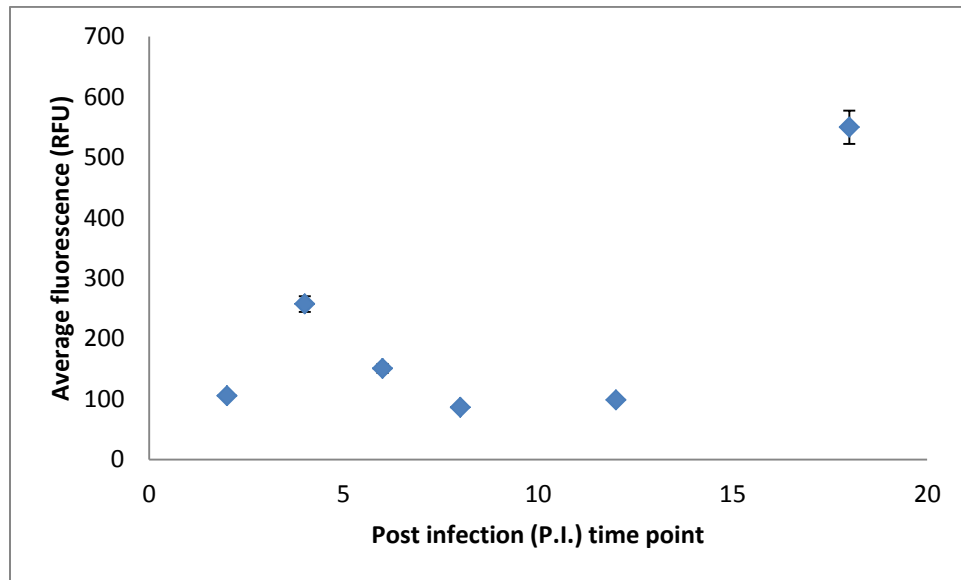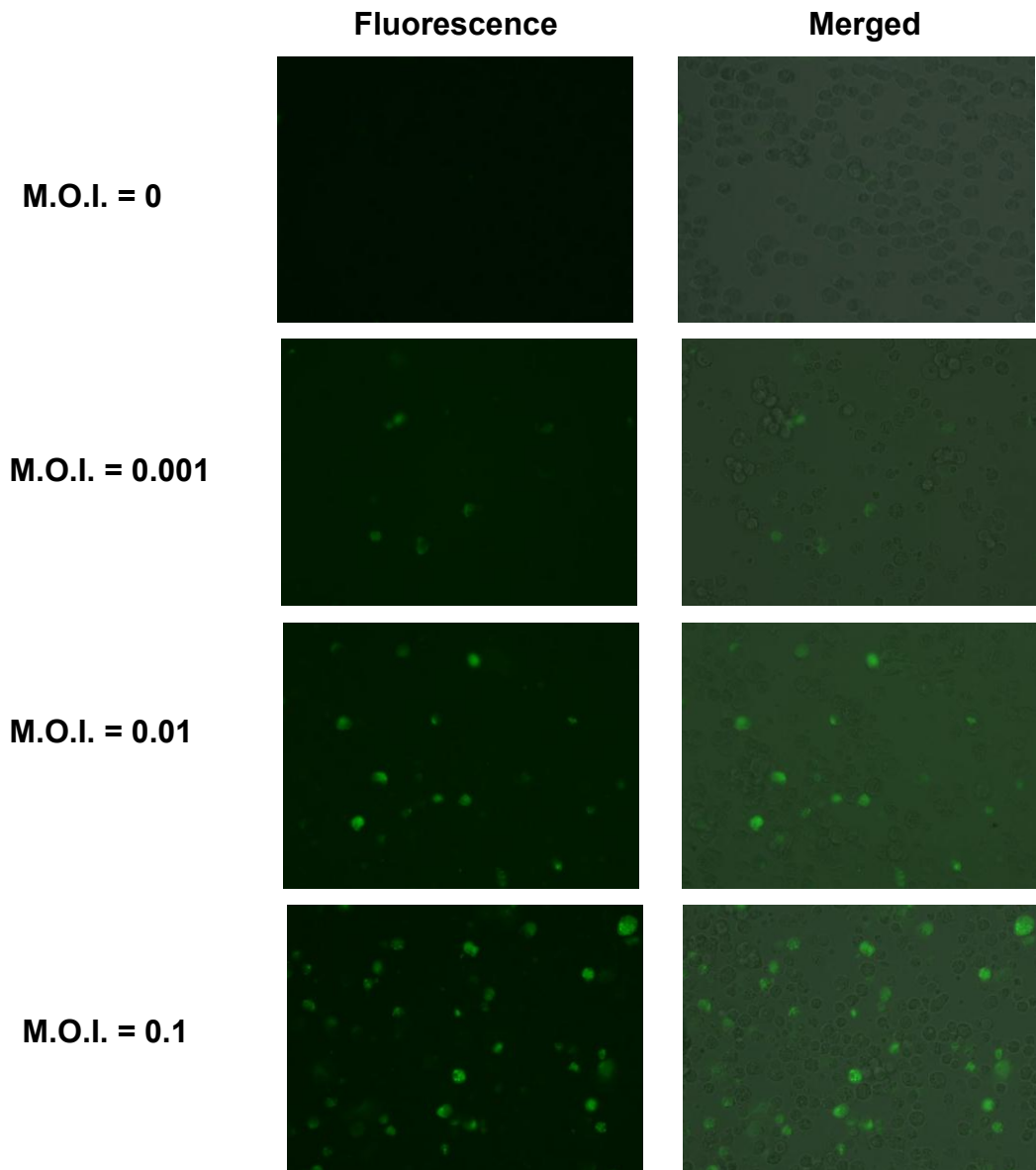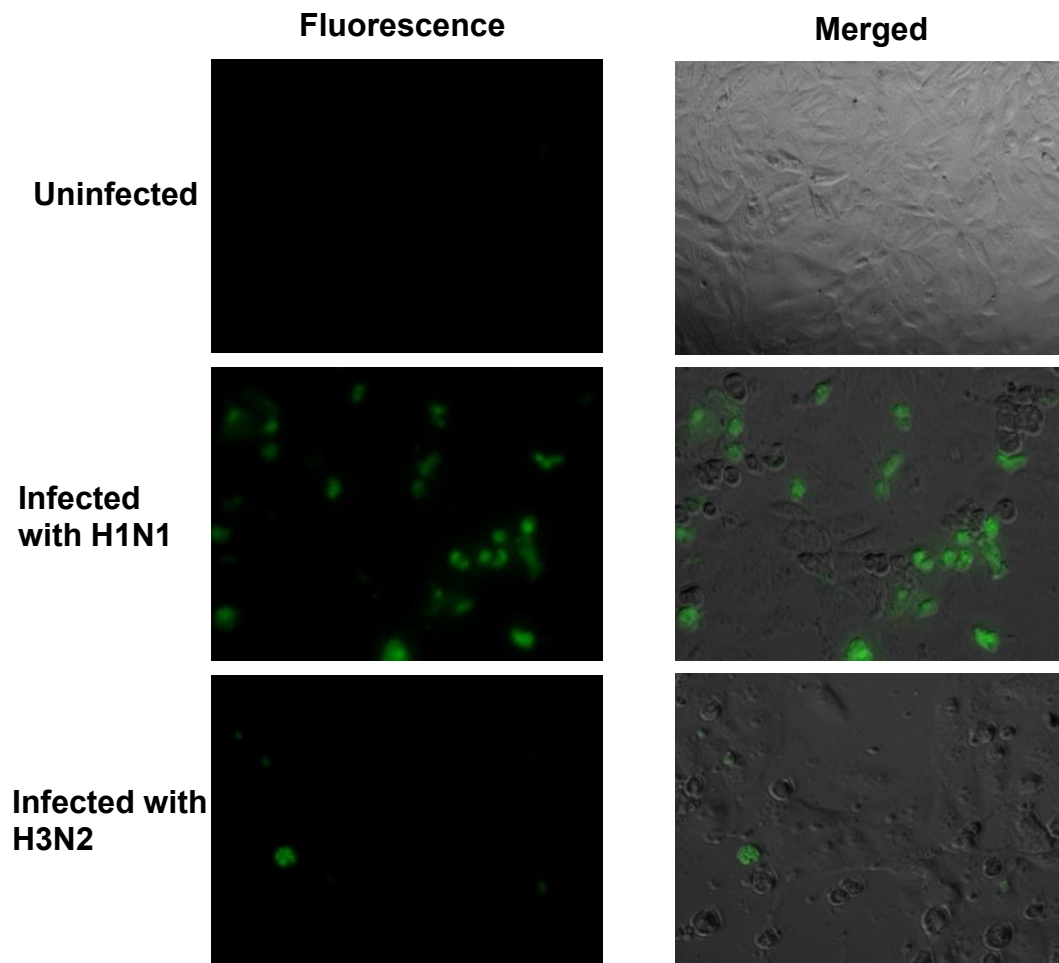**Fig. 3.1.**

Fig. 3.2.

	Fluorescence	Merged
UNINFECTED		
T = 2.5 hr		
T = 4 hr P.I.		
T = 8 hr P.I.		
T = 12 hr P.I.		
T = 18 hr P.I.		

Fig. 3.3.

Fig. 3.4.

	Fluorescence	Merged
M.O.I. = 0		
M.O.I. = 0.001		
M.O.I. = 0.01		
M.O.I. = 0.1		

Fig. 3.5.

Fig. 3.6.

Fig. 3.7.

T = 0 sec **T = 30 sec** **T = 1 min**

T = 5 min **T = 15 min** **T = 30 min**
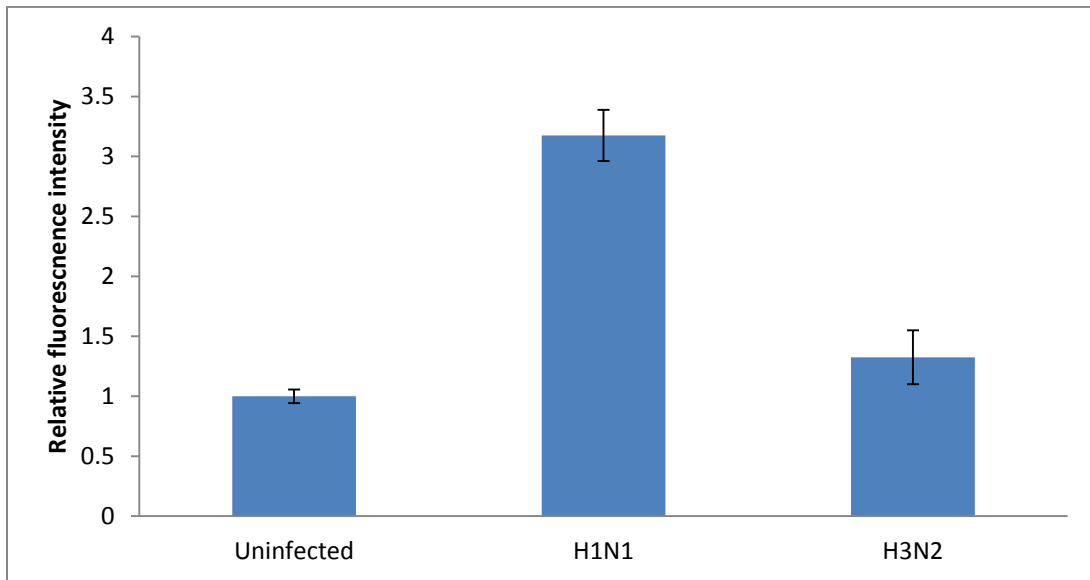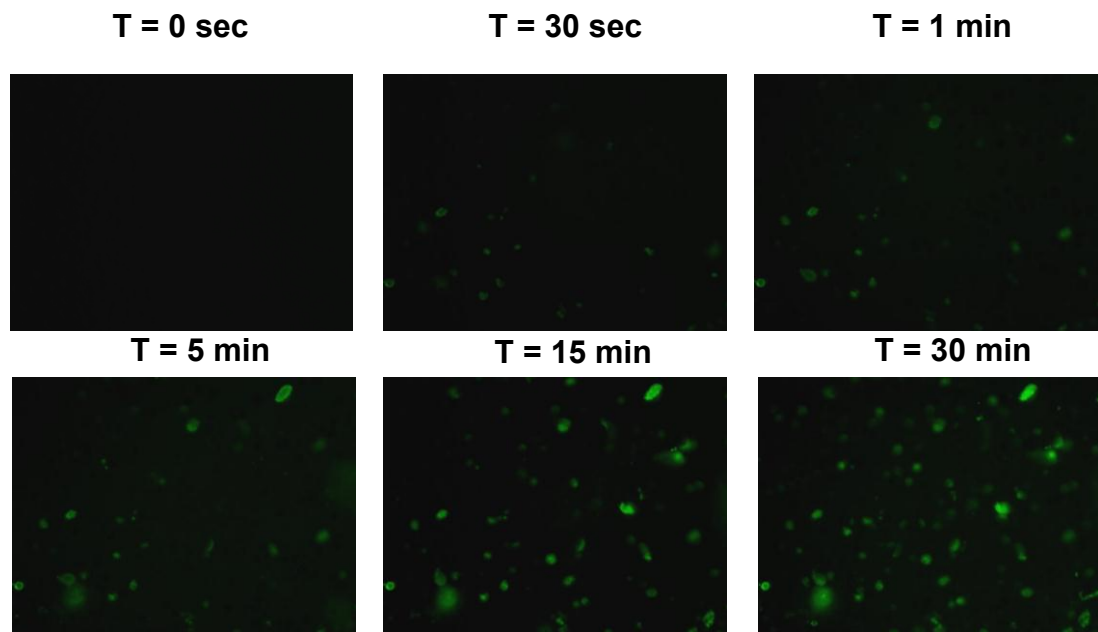
Chapter 4

A Quantum dot based protein module for the detection of viral protease and development of anti-viral agents

Abstract

Proteases are involved in many essential cellular processes such as blood coagulation, fibrinolysis, hormone maturation, and apoptosis. They are also used as the key virulence factors for pathogenic infection. As a result, many proteases have been employed as a main target for drug development and disease diagnostics. One of the most promising methods for probing protease activity is based on the principle called fluorescence resonance energy transfer (FRET) containing two fluorophores located less than 100 Å apart. In this chapter, we develop a genetically engineered protein module that is designed with 1) a quantum dot (QD)-binding moiety containing hexa-histidine, 2) a cysteine site for fluorescent dye incorporation, 3) a protease cleavage site, 4) an elastin-like protein (ELP) domain for thermal purification, and 5) a flanking TAT peptide sequence for cell penetration. The advantages of this approach include the significant reduction of cost on peptide synthesis, easy modulation of the placement of target sequence and intracellular monitoring of viral protease activity. We investigated the use of these QD-based FRET substrates for the detection of poliovirus 2A protease in living cells. This assay provides a sensitive and quantitative measure of viral protease activity *in vivo* and the capability of this cell-based platform to be used for high throughput screening of viral protease inhibitors was demonstrated.

Introduction

Proteases are enzymes that hydrolyze polypeptides or proteins by cleaving their peptide bonds. These enzymes are involved in many essential cellular processes (1) as well as being used as the key virulence factors for pathogenic infection (2). These properties make proteases a prime target for detailed investigation to better understand the disease development process and to identify targets for drug treatment.

One of the most promising methods for probing protease activity is based on the principle of fluorescence resonance energy transfer (FRET) (3-5). The theory is based on two organic fluorophores that are less than 100 Å apart, linked by a protease cleavage sequence thereby enabling transfer of energy from donor to acceptor. Cleavage of the linker peptide separates the donor and acceptor, resulting in an increase in the emission intensity of the donor and a reduction in the acceptor emission. This change in fluorescence can be directly correlated to the activity of the protease. Efforts to adapt this FRET-based method for probing *in vivo* protease activity have been demonstrated by using genetically engineered fluorescent protein (CFP-YFP) pairs as FRET donors and acceptors (6-7). However, the process of producing stable, genetically engineered cell lines expressing protease FRET substrates is a tedious task, and a more feasible alternative to introduce FRET probes inside living cells is required. Also, one of the major downsides to using organic fluorophores is their low resistance to photo degradation thereby making them unsuitable for long term monitoring in living cells (8).

To address some of the functional limitations encountered by organic fluorophores, a new class of inorganic fluorophores known as quantum dots (QDs) have been explored as an energy donor (9-11). QDs are luminescent semiconductor nanocrystals that exhibit excellent optical properties such as narrow emission, broad excitation, high quantum yield and high resistance to photo degradation. Recently, FRET-based protease assays have been successfully demonstrated using QDs as the energy donor (12). A synthetic peptide was designed containing an N-terminal hexahistidine (His6) for conjugation to QD and a C-terminal cysteine for Cy3 attachment. Cleavage of this synthetic linker peptide by the protease thrombin resulted in the disruption of FRET causing an increase in the QD emission. However, the use of synthetic peptides as FRET substrates is expensive and purification of the protein-dye conjugates requires tedious binding, washing and elution steps making it difficult to be configured in a high-throughput setting. Ideally, a method that provides easy production, purification and conjugation of the peptide substrate to acceptor dyes and QDs is necessary to provide a low-cost and tunable approach for monitoring protease activity in living cells.

To address some of the drawbacks of the above mentioned methods, we have previously designed a genetically programmable module that can be easily adapted for probing the activity of a wide range of proteases (13). The approach was to generate a QD-modified, protease-specific protein module that can be used as a FRET substrate for monitoring intracellular protease activity. The protein module (Figure 4.1.) is composed of 1) an N-terminus histidine tag (His) for conjugation with quantum dot via strong

metal-affinity coordination bond with the Zn^{2+} on the shell, 2) a protease cleavage site, 3) a unique cysteine site for fluorescent dye incorporation based on thiol-maleimide interaction , 4) an ELP domain for thermally triggered purification based on ELP's ability to undergo reversible phase transition from water soluble form into aggregates (14), and 5) a flanking TAT peptide sequence for the intracellular delivery of the substrates (15-17). The feasibility of the approach to monitor the *in vivo* progress of protease activity has been demonstrated using the HIV-1 protease as the target (13). By exploiting the modular nature of the probe design, we demonstrate the detection of poliovirus infection and the screening of protease inhibitors by using the poliovirus 2A protease (PV2A) as a target.

Materials and Methods

Design of protein module

The genetically programmable protein module, His6-1D2Apeptide-Cys-ELP105K-Tat was designed with 1) a hexa-histidine tag as the QD binding moiety via metal affinity binding, 2) the 1D2A cleavage site (STKDLTTYGFGHQNKA) for the poliovirus 2A protease, 3) a unique cysteine residue for site-specific conjugation with a Alexa 568 maleimide dye, 4) an ELP domain [(VPGVG)2VPGKG(VPGVG) 2]21 for reversible phase purification, and 5) a flanking TAT peptide sequence (GGTKTGRRRQRRKKRGY) for intracellular delivery.

Expression and purification of peptides

To construct an expression vector for His6-PV2A-Cys-ELP105K-TAT, the procedure described by Lao et al (18) was followed and the vector was constructed by Seung Hyun Kang. For protein expression, *E.coli* BL-21 (DE3) (Novagen) transformed with plasmid pET-H-PV2A-ET was grown in terrific broth media containing 100ug/ml ampicillin at 37°C until an optical density (O.D.) at 600nm reached 0.5. The flasks were then transferred to 30°C for expression. When the O.D. reached 5, cells were harvested by centrifugation, resuspended in 50mM Tris/HCl (pH 8.0) with 0.1M Na Cl and 1mg/ml of lysozyme and lysed by sonication. Cell debris was removed by centrifugation at 16,000 g for 30 min. Proteins were purified by three rounds of temperate transition cycles as described previously (19). Briefly, for each cycle, NaCl was added to the sample at a

final concentration of 2M and the sample was heated to 37°C and centrifuged at 16,000 g at 30°C for 15 min. The pellet containing the proteins were resuspended in ice-cold 50mM Tris/HCl (pH 8.0) with 0.1M NaCl and centrifuged at 16,000 g at 4°C for 15 min to remove undissolved proteins. This temperature transition cycle was repeated once more, and the pellet containing H-PV2A-ET was finally resuspended in ice cold 50mM Tris/HCl (pH 8.0) with 0.1M NaCl. The purity of the protein was confirmed by SDS-PAGE at the expected molecular weight of 48 kD.

Conjugation of peptide with fluorescent dye

The labeling of protein with a thiol reactive dye was performed by slight modification of the procedure illustrated by Massodi et al. (20). Purified proteins were resuspended in 50mM potassium phosphate buffer (pH 7) at a final concentration of 40µM. Tris-(2-carboxyethyl) phosphine (TCEP) and Alex 568 maleimide, a thiol reactive dye, were added to a 10-fold and 2-fold molar excess, respectively. The mixture was then incubated and rotated for 2 hr at room temperature in the dark. The reaction was stopped and the unreacted dyes were removed by two or three thermal precipitation cycles as described in the protein purification procedure. The degree of labeling of the protein was calculated using the formula:

$$\frac{A_x}{\varepsilon} \times \frac{MW \text{ of protein}}{mg \text{ protein/ml}} = \frac{moles \text{ of dye}}{moles \text{ of protein}}$$

Where A_x is the absorbance value of the dye at the absorption maximum wavelength and ε is the molar extinction coefficient of the dye.

Assembly of Quantum dot-protein-dye conjugate

Tri-octyl phosphine oxide (TOPO) capped CdSe-ZnS quantum dots with an emission maximum at 545nm (QD 545) were purchased from Evident Tech. Inc. The quantum dots were suspended in an inorganic solvent and to utilize them for biological applications, a cap exchange with dihydrolipoic acid (DHLA) (Sigma-Aldrich) was necessary to make them hydrophilic. The basic procedure followed for DHLA cap exchange is described by Clapp et al (21). After QD surface replacement, the DHLA-capped QDs were resuspended in 10mM Hepes buffer. The conjugation of QDs to fluorophore-labeled protein module to complete the FRET pair was adapted from (21). DHLA-capped QDs (390nM) were added to Alexa568-labeled proteins that were resuspended in 10mM HEPES buffer (pH 8.2) at 1:1 to 1:50 ratio of QDs to protein module. The samples were mixed thoroughly and incubated at room temperature for overnight. After conjugation, the FRET efficiency was measure using a fluorometer (Synergy 4, BIOTEK Instruments) by exciting at 430nm and the spectrum was recorded from 475nm to 650nm.

Hela Cell Culture

HeLa cells were obtained from American Type Culture Collection (ATCC) and cultured in autoclavable Eagle's minimal essential medium (AMEM) with Earle's salts (Irvine Scientific, Santa Ana, CA) containing 0.075% $NaHCO_3$, 10mM nonessential amino acids (NEAA; Gibco BRL, Grand Island, NY), 2mM L-glutamine (Hyclone, Logan, UT), 20mM HEPES (pH 7.4), 100 mg/ml penicillin, 100U/ml streptomycin (Hyclone) and 8%

(vol/vol) fetal bovine serum (FBS; Hyclone) and buffered with. Cells were grown in an incubator maintained at 37°C and 5% (vol/vol) CO_2. Phosphate-buffered saline solution (PBS; 0.01M phosphate, pH 7.4, 0.138 M Na Cl, and 2.7mM KCl) and Tris-buffered saline solution (TBSS; 0.05M Tris, pH 7.4, 0.28 M NaCl, 10mM KCl, and 0.82mM Na_2HPO_4) were used during the washing steps for HeLa cell culture.

Virus preparation

Poliovirus type 1(PV1) (strain LSc) was obtained from American Type Cell Culture (ATCC VR-59) and propagated in HeLa cells for upto 5 days at 37°C. The virus stock was harvested and purified by freeze-thaw method and extracting the cell lysate with chloroform. The fresh virus stock is stored as 500µl aliquots at -80°C until use.

Plaque assay

The PV1 virus stock was thawed and then a series of 10-fold serial dilutions in 1X PBS were prepared. HeLa cells that were 90% confluent and 1-day old and grown in 12-well, 22.1mm dishes (Costar;Corning) were infected with 1ml of virus dilution. After 90min of adsorption at room temperature, the solutions were aspirated and 1ml of 2% carboxymethylcellulose (CMC) sodium salt (Sigma-Aldrich) containing 100mL of 2X AMEM (Irvine Scientific) with 2mL of 7.5% $NaHCO_3$, 4mL of 1M Hepes, 2mL of NEAA, 5mL of A/B-L, and 4mL of FBS (Sigma-Aldrich) was added to each well. After 5 days of incubation at 37°C, the CMC layer was removed and the cells were stained and fixed with 0.8% crystal violet and 3.7% formaldehyde solution for 2 hours. The excess

stain was removed by washing with de-ionized water and virus plaques were counted to calculate the titre of the stock.

Intracellular delivery of probes, infection with PV1 and inhibitor treatment

HeLa cells were seeded into 96 well clear bottom black wall side plates (Nunc Scientific) at 37°C in 5% CO_2 in air and cultured to 90% confluency. After removing the incubation medium, the cell monolayer was washed twice with 1X PBS. Cells were then incubated at 37°C in the dark with 1X Leibovitz L-15 medium (Invitrogen) containing QD-PV2A-Alexa568 at QD concentrations of 150nM for 2 hrs. After 2 hr incubation with the probes, the cells were washed with PBS; resealed with Leibovitx medium and observed under Zeiss Axiovert 40 CFL inverted fluorescence microscope. To infect with PV1, the HeLa cell monolayer was washed twice with 1 X phosphate buffered saline solution (PBS) and incubated with different concentrations of PV1. The virus was allowed to adsorb to the cell surface for 30min at 37°C then the unbound virus particles are removed. The infection was allowed to proceed for 12hrs and the cells were then observed under fluorescence microscope. For experiments that required the treatment of HeLa cells with protease inhibitors, the culture medium was removed by aspiration and the virus suspension in 1X PBS with different concentrations of N-methoxysuccinyl-Ala-Ala-Pro-Val-chloromethylketone (MPCMK) (Sigma–Aldrich), a known PV2A protease inhibitor was added to each well.

Fluorescence Microscopy and image processing

Cell imaging was performed on a Zeiss Axiovert 40 CFL inverted microscope equipped with a 12-V, 35-W halogen lamp (for phase contrast images) and an HBO 50 W/AC mercury lamp (for fluorescence images). The objective used were a 5x/0.12 A-Plan, 10x/0.25 A-Plan, a 20x/0.50 EC Plan-NEOFLUAR, and a 40x/0.50 LD A-Plan (Zeiss). Fluorescent probes were detected by using two different filter sets; QD filter consisting of a D436nm exciter, D535/50nm emitter, and a 475nm dichroic long pass beam splitter (Chroma Technology) and FRET filter consisting of a D 436nm exciter , a D610/50nm emitter and a 475nm dichroic long pass beam splitter. Images were acquired by using a ProgRes MFscan Monochrome CCD camera (Jenoptik). Both phase contrast and fluorescence images were analyzed by using Image-Pro-PLUS software (Media Cybernectics). All settings for image processing were kept constant and exposure times were kept consistent throughout the course of the experiment. The intracellular distribution of the QD-based probes was analyzed by merging the bright field images with the fluorescence images. Composite merged images were produced by superimposing the fluorescence images from the QD filter and from the FRET filter.

Quantification of Fluorescent Signals

The QD fluorescence intensity and Alexa fluorescence intensity for each well was measured by randomly choosing six to seven fields within each well of treated or untreated samples using Image-Pro PLUS analysis software.

Results and Discussion

Assembly and characterization of QD-peptide-dye conjugates

The purified protein module (H-PV-ET) was labeled with a thiol-reactive dye - Alexa 568 maleimide through the formation of a thioether bond with a unique cysteine residue that was incorporated after the 1D2A substrate sequence. This particular dye was chosen based on the overlapping optical spectra between the DHLA-capped CdSe/ZnS QD (QD 540) and Alexa-568. The dye was successfully conjugated to the protein module and the presence of the ELP domain enabled the separation of unreacted dyes using thermally triggered precipitation rather than conventional expensive methods such as desalting column or dialysis. After three cycles of purification, the free dye was removed in the supernatant and fluorescence was only visible in the pellet containing the H-PV-ET-Alexa dye conjugates, confirming the efficiency of the thermal precipitation. The commercially purchased TOPO capped quantum dots were made water soluble by exchanging the surface ligands with DHLA. The QD emission at 540nm was measured before and after DHLA capping (Figure 4.2.) and a red shift of 10nm was observed as reported previously (22). To generate the functional FRET pair, QDs were self-assembled onto the H-PV-ET-Alexa dye conjugates via metal-affinity interaction between the histidine tag and the ZnS shell of the QD. Figure 4.3. shows the spectra for the QD540 self-assembled with different ratios of H-PV-ET-Alexa. As expected, binding of QDs to H-PV-ET-Alexa dye conjugates resulted in a sharp decline in the QD emission and a corresponding increase in the Alexa 568 intensity. This result confirms the correct

assembly of H-PV-ET-Alexa conjugates onto QD surface resulting in the efficient quenching of the QD via FRET. A conjugation ratio of 10 was chosen for subsequent studies since it offers a good FRET ratio and cleavage of a small number of target protease sequences should result in a large, detectable change in the FRET efficiency.

Intracellular delivery of QD-PV-Alexa probes

To investigate the ability of the TAT peptide sequence to deliver the QD-H-PV-ET-Alexa probes into living cells, a monolayer of HeLa cells was incubated with the probes for 2 hours and subsequently washed to remove any unbound particles. The cells were imaged using a fluorescent microscope containing a QD (436nm/535nm) (green fluorescence) and an Alexa (436nm/610nm) (red fluorescence) filter set. The fluorescent images from both channels were merged and a composite image was created by merging the fluorescent images with a DIC image (Figure 4.4.). The composite image clearly showed the localization of the probes inside the cells indicating successful translocation of the cargo via TAT peptide based delivery. In contrast, incubation of unconjugated QDs resulted in no substantial uptake within the same duration, confirming that the TAT sequence presented on the protein module was fully functional and solely responsible for the intracellular uptake (data not shown). It was also observed that the fluorescent signal from the Alexa filter was much higher than the QD filter which was consistent with our *in vitro* fluorescent measurements. The intracellular fluorescent intensity was constant for up to 24 hrs, confirming that the probes were retained inside the cells and resistant to intracellular degradation.

Detecting PV2A protease activity in HeLa cells

To demonstrate the ability of the probes to monitor PV2A protease activity in individual cells, a confluent monolayer of HeLa cells was incubated with 150nM of QD-H-PV-ET-Alexa probes for 2 hrs and washed to remove the unbound particles. The cells were then infected with 10 fold serial dilutions of PV and the infection was allowed to proceed for 12 hrs. Fluorescent images were acquired 12 hrs P.I. and a significantly higher number of green cells were observed for the sample infected with the highest PFU (10^5 PFU) while fluorescent signals remained unchanged for uninfected (control) cells (Figure 4.5.). Also, the number of cells showing an increase in the QD signal was in accordance with the dosage of the virus used for infection. This further validated our observation that the changes in FRET signal was a result of cleavage of the target sequence by the viral protease (PV2A). The ability of this platform to be used as a detection method for viral protease was demonstrated by quantifying the QD and Alexa signals using the Image-Pro PLUS software. The total QD fluorescence intensity (FD) and Alexa fluorescence intensity (FA) was measured for each well (uninfected, different dosages of infection) and the FRET ratio was calculated. Figure 4.6. shows a plot of FA/FD ratio against varying infectious dosages where the control cells have a high FRET ratio of 8.09 due to the energy transfer from the QD to Alexa568 dye. In comparison, the FA/FD ratio gradually decreased to 1.88 when the infectious dose was increased from 1PFU to 10^5 PFU due to the disruption of FRET. Hence, the QD-based FRET assay system provides a simple, rapid and convenient way of detecting viral infection *in vivo* by directly monitoring the proteolytic activity.

PV2A protease inhibition assay using QD-PV-Alexa probes

To further confirm that this disruption in FRET was a protease-specific event and to evaluate usage of this FRET module for screening of protease inhibitors, a similar *in vivo* infection experiment was repeated in the presence of a protease inhibitor. The cells were treated with different concentrations of N-methoxysuccinyl-Ala-Ala-Pro-Val-chloromethylketone (MPCMK), a selective inhibitor of the poliovirus 2A protease (23). MPCMK has been previously used as a positive control for screening of biomolecules as potential anti-viral agents using a similar cell-based assay technique (24). From Figure 4.7., it was observed that the inhibitor induced a dose dependent decrease in the number of cells showing an increased QD signal. Cells that were untreated with the inhibitor showed a high increase in QD signal as observed from the previous experiment. The highest inhibitor dosage of 1μM was shown to completely inhibit the PV2A protease activity and the resulting merged image was virtually the same as that obtained from the control cells. To quantify the inhibition effect of MPCMK on PV2A protease, QD and Alexa fluorescent signals were measured using Image-Pro-PLUS software. The total QD fluorescence (FD) intensity and Alexa fluorescence (FA) intensity for each well (uninfected, infected and different dosages of MPCMK) was quantified. In Figure 4.8., the FA/FD ratio was plotted against different MPCMK concentration where control cells show a high FRET ratio of 8.06 due to the energy transfer from the QD to Alexa568 dye. In comparison, the FA/FD ratio decreased to 1.22 due to the disruption of FRET when the cells were infected with a high dosage (10^5 PFU) of the virus. There was a gradual recovery in the FRET ratio with the increasing dose of the inhibitor and at a

concentration of 1μM, the FA/FD ratio was nearly completely recovered. The FA/FD ratio of the inhibitor was used to calculate the percent inhibition by using the following equation: (Inhibitor treated − Untreated) / (Uninfected − Untreated) * 100. As seen in Figure 4.9., a dose response curve was generated and the IC-50 value of MPCMK was determined to be 0.3μM. The IC-50 value of MPCMK determined using our QD based assay system was similar to the value reported by other methods (25-26). Hence, we can conclude that we have validated the potential of using this QD based FRET assay system for rapid and sensitive screening of other viral protease inhibitors.

References

1. Neurath, H. 1999. Proteolytic enzymes, past and future. *Proc. Natl. Acad. Sci. U.S.A.* 96:10962–10963.

2. Shao, F., P. M. Merritt, Z. Bao1, R.W. Innes, and J. E. Dixon. 2002. A Yersinia effector and a Pseudomonas a virulence protein define a family of cysteine proteases functioning in bacterial pathogenesis. *Cell.* 109:575-588.

3. Zhang, B. 2004. Design of FRET-based GFP probes for detection of protease inhibitors. *Biochem. Bioph. Res.Co.* 323:674-678.

4. Mitra, R. D., C. M. Silva, and D. C. Touvan. 1996. Fluorescence resonance energy transfer between blue-emitting and red-shifted excitation derivatives of the green fluorescent protein. *Gene*. 173:13-17.

5. Pennington, M. W., and N. A. Thornberry. 1994. Synthesis of fluorogenetic interleukin-1-beta converting enzyme substrate based on resonance energy transfer. *Pept. Res*. 7:72-76.

6. Hwang, Y.-C., W. Chen, and M. V. Yates. 2006. Using Fluorescence Resonance Energy Transfer for Rapid Detection of Enteroviral Infection In Vivo. *Appl. Environ. Microbiol.* 72:3710-3715.

7. Heim, R., and R. Y. Tsien. 1996. Engineering green fluorescent protein for improved brightness, longer wavelengths and fluorescence resonance energy transfer. *Curr. Biol.* 6:178-182.

8. Hermanson, G. T. 1996. Bioconjugate Techniques; Academic Press: London; Chapter 8.

9. Bruchez, M. Jr, M. Moronne, P. Gin, S. Weiss, and A. P. Alivisatos. 1998. Semiconductor nanocrystals as fluorescent biological labels. *Science.* 281:2013-2016.

10. Michalet, X., F. F. Pinaud, L. A. Bentoila, J. M. Tsay, S. Doose, J. J. Li, G. Sundaresan, A. M. Wu, S. S. Gambhir, and S. Weiss. 2005. Quantum dots for live cells, in vivo imaging, and diagnostics. *Science*. 307:538-544.

11. Medintz, I. L., A. R. Clapp, H. Mattoussi, E. R. Goldman, B. Fisher, and J. M. Mauro. 2003. Self-assembled nanoscale biosensors based on quantum dot FRET donors. *Nat. Mater.* 2:630-638.

12. Medintz, I. G., A. R. Clapp, F. M. Brunel, T. Tiefenbrunn, H. T. Uyeda, E. L. Chang, J. R. Deschamps, P. E. Dawson, and H. Mattoussi. 2006. Proteolytic activity monitored by fluorescence resonance energy transfer through quantum-dot-peptide conjugates. *Nat. Mater.* 5:581-589.

13. Biswas, P., L. N. Cella, S. H. Kang, A. Mulchandani, M. V. Yates and W. Chen. 2011. A quantum-dot based protein module for in vivo monitoring of protease activity through fluorescence resonance energy transfer. *Chem. Commun.* 47: 5259-5261.

14. Urry, D. W. 1997. Physical Chemistry of biological free energy transduction as demonstrated by elastic protein-based polymers. *J. Phys. Chem. U.S.*101:11007-11028.

15. Gupta, B., T. S. Levchenko, and V. P. Torchilin. 2005. Intracellular delivery of large molecules and small particles by cell-penetrating proteins and peptides. *Adv. Drug Deliver. Rev.* 57:637– 651.

16. Lewin, M., N. Carlesso, C. Tung, X. Tang, D. Cory, D. T. Scadden, and R. Weissleder. 2000. Tat peptide-derivatized magnetic nanoparticles allow in vivo tracking and recovery of progenitor cells. *Nat. Biotechnol.* 18:410-414.

17. Deschayes, S., M. C. Morris, G. Divita, and F. Heitz. 2005. Cell-penetrating peptides: Tools for intracellular delivery of therapeutics. *Cell. Mol. Life. Sci.* 62:1839-1849.

18. Lao, U. L., A. Chen, M. R. Matsumoto, A. Mulchandani, and W. Chen. 2007. Cadmium Removal from Contaminated Soil by Thermally Responsive Elastin (ELPEC20) Biopolymer. *Biotechnol. Bioeng.* 98:349-355.

19. Kim, J.-Y., S. O'Malley, A. Mulchandani, and W. Chen. 2005. Genetically engineering elastin-protein A fusion as a universal platform for homogenous, phase-separation immunoassay. *Anal. Chem.* 77:2318-2322.

20. Massodi, I., G. L. Bidwell, and D. Raucher. 2005. Evaluation of cell penetrating peptides fused to elastin-like polypeptide for drug delivery. *J. Control. Release*. 108:396-408.

21. Clapp, A. R., E. R. Goldman, and H. Mattoussi. 2006. Capping of CdSe-ZnS quantum dots with DHLA and subsequent conjugation with proteins. *Nat. Protoc.* 1:1258-1266.

22. Algar, W. R., and U. J. Krull. 2007. Luminescence and stability of aqueous thioalkyl acid capped CdSe/ZnS quantum dots correlated to ligand ionization. *Chemphyschem.* 8:561-568.

23. De Palma, A. M., I. Vliegen, E. De Clercq, and J. Neyts. 2008. Selective inhibitors of picornavirus replication. *Med. Res. Rev.*6:823-884.

24. Hwang, Y.-C, J. J.-H. Chu, P. L. Yang, W. Chen, and M. V. Yates. 2008. A Cellular Sensor for Screening Small Molecules Suppressing Poliovirus Replication. *Antivir. Res.* 77:232–236.

25. Belov, G. A., P. V. Lidsky, O. V. Mikitas, D. Egger, K. A. Lukyanov, K. Bienz, and V. I. Agol. 2004. Bidirectional Increase in Permeability of Nuclear Envelope upon Poliovirus Infection and Accompanying Alterations of Nuclear Pores. *J. Virol.* 78:10166-10177.

26. Molla, A., C. U. T. Hellen, and E.Wimmer. 1993. Inhibition of Proteolytic Activity of Poliovirus and Rhinovirus 2A Proteinases by Elastase-Specific Inhibitors. *J. Virol.* 67:4688-4695.

Legends to Figures

Fig. 4.1. Schematic representation of the self-assembled QD-peptide nano-biosensor containing engineered protein module H-PV2A-ET. The protein module H-PV2A-ET contains hexahistidine, PV2A cleavage sequence (1D2A), cysteine residue for dye incorporation, ELP for thermal purification and cell penetrating Tat peptide. The QD fluorescence is quenched due to FRET. In the presence of a target viral protease, FRET is disrupted causing an increased QD signal thus enabling a simple activity assay.

Fig. 4.2. Fluorescence emission of TOPO capped and DHLA capped QD. 1μM samples of TOPO-QD and DHLA-QD were excited at 435nm and emission spectra were measured using a spectrofluorometer.

Fig. 4.3. Fluorescence emission spectra of QD-PV-Alexa assemblies at various QD: Alexa ratios. Samples were excited at 435nm.

Fig. 4.4. Cellular uptake of QD-PV-Alexa probes. Representative images of HeLa cells incubated for 2 hr with 150nM QD-PV-Alexa probes. The cells were visualized with a fluorescence microscope at 435ex/535em for QD and 435ex/610em for FRET. The images obtained using QD and FRET filter sets were merged. DIC images of cells were also taken. The DIC images were merged with merged fluorescence image to obtain corresponding merged composite fluorescent images.

Fig. 4.5. Detection of PV2A viral protease in HeLa cells using QD based FRET assay system. QD-PV-Alexa probes were delivered into HeLa cells for 2 hr. HeLa cells were

then infected with poliovirus-1 (PV1) with varying dosage from 0 PFU to 10^5 PFU. 12 hr P.I., cells were observed under fluorescence microscope at 435ex/535em for QD and 435ex/610em for FRET. The images obtained using QD filter and FRET filter were merged. Only merged fluorescent images are shown for control (uninfected) and each dosage of the virus.

Fig. 4.6. Quantitative analysis of PV2A activity using QD based FRET assay system. The total fluorescence intensity of images obtained using QD filter (FD) and FRET filter (FA) for control and different dosages of infection was quantified using Image-Pro-PLUS software. The FA/FD ratio for each set of images was calculated and plotted against PV1 infectious dose.

Fig. 4.7. Monitoring the inhibition efficiency of PV2A protease inhibitor MPCMK using QD-PV-Alexa based FRET assay system. QD-PV-Alexa probes were delivered into HeLa cells for 2 hr. HeLa cells were then treated with increasing dose of MPCMK inhibitor (0.06 to 1µM) and infected with PV1 at 10^5 PFU. 12 hr P.I., cells were observed under fluorescence microscope at 435ex/535em for QD and 435ex/610em for FRET. The images obtained using QD filter and FRET filter were merged. Only merged fluorescent images are shown for control (uninfected), infected and inhibitor treated cells.
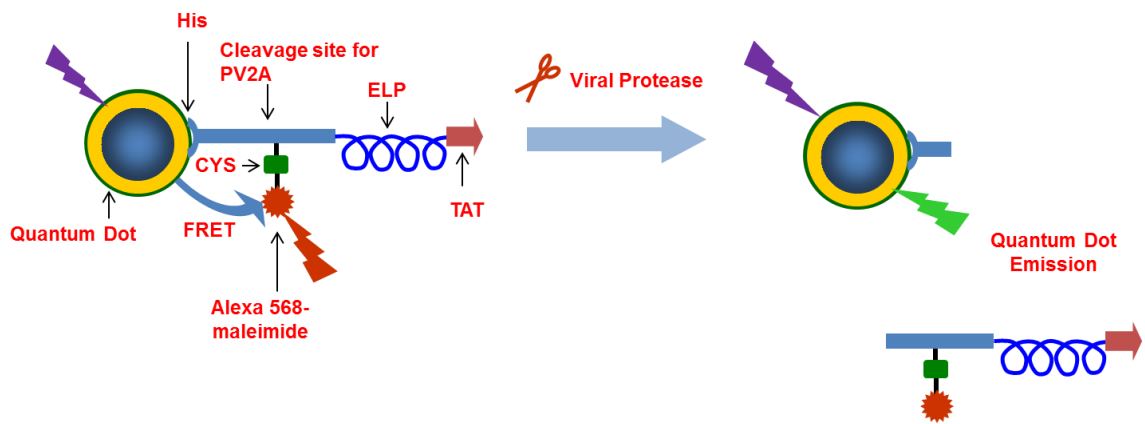
Fig. 4.8. Quantitative analysis of MPCMK inhibition using QD based FRET assay system. The total fluorescence intensity of images obtained using QD filter (FD) and FRET filter (FA) for control and inhibitor treated cells was quantified using Image-Pro-
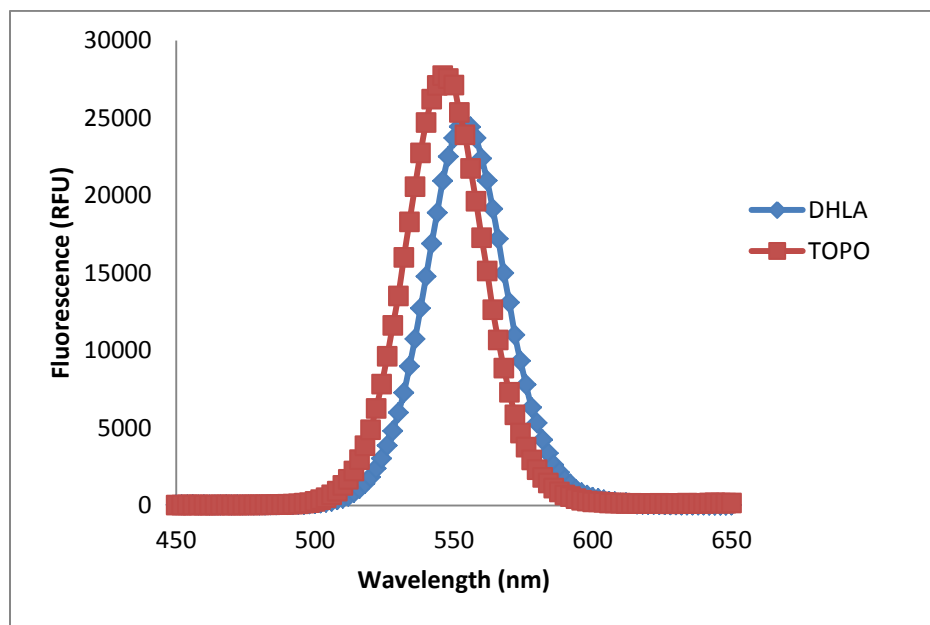
PLUS software. The FA/FD ratio for each set of images was calculated and plotted MPCMK inhibitor concentrations.

Fig. 4.9. Percent inhibition in PV2A protease activity with MPCMK inhibitor using QD-PV-Alexa FRET system. The FA/FD ratio of each sample was used to calculate the percent inhibition in protease activity by using the equation: (Inhibitor treated – Untreated)/ (Uninfected – Untreated) *100.
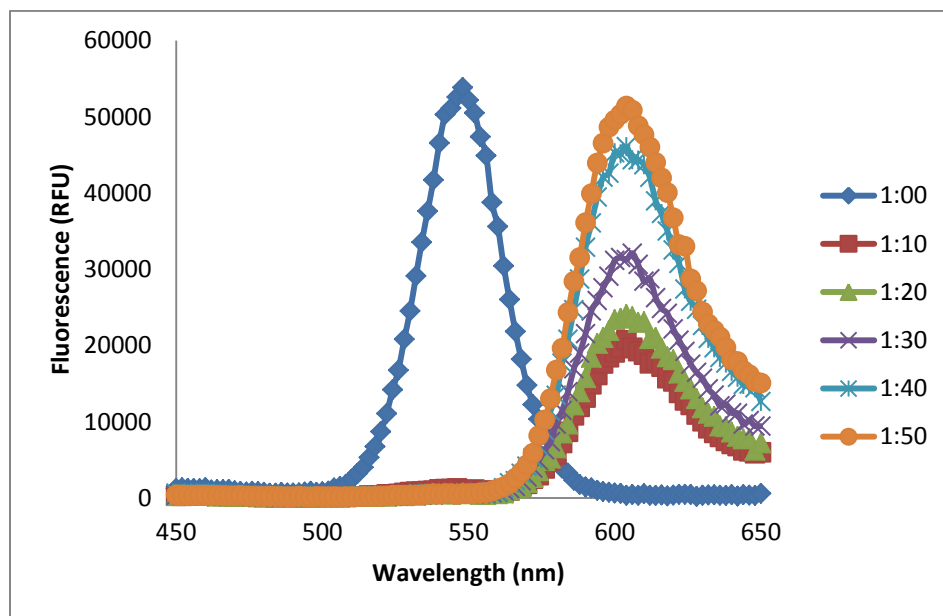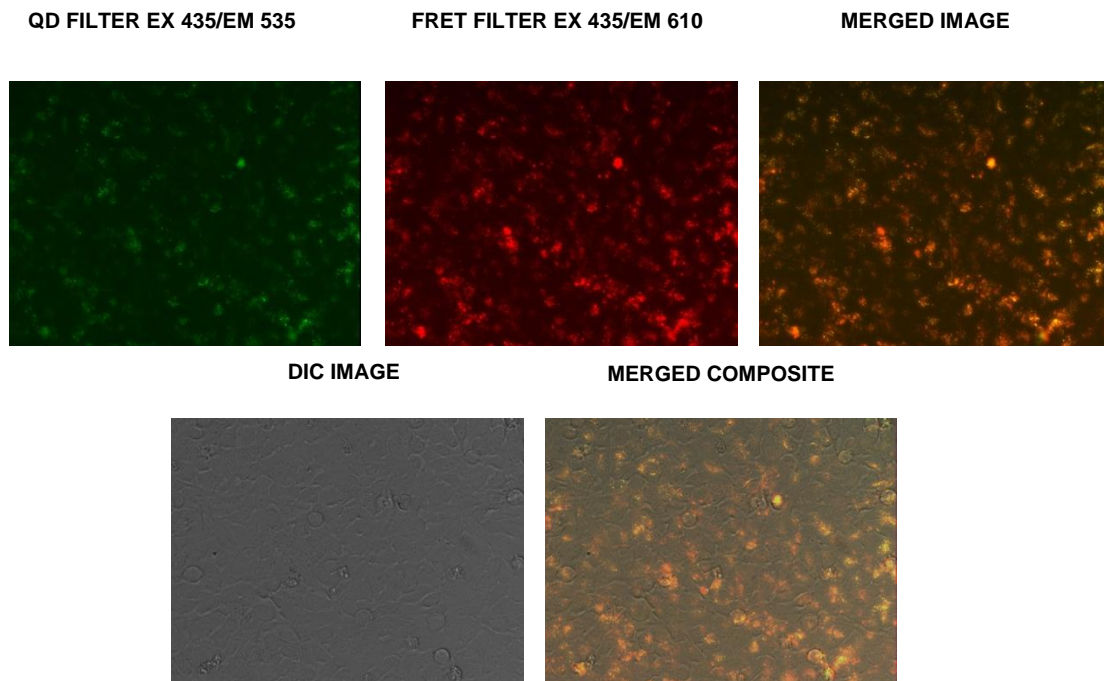
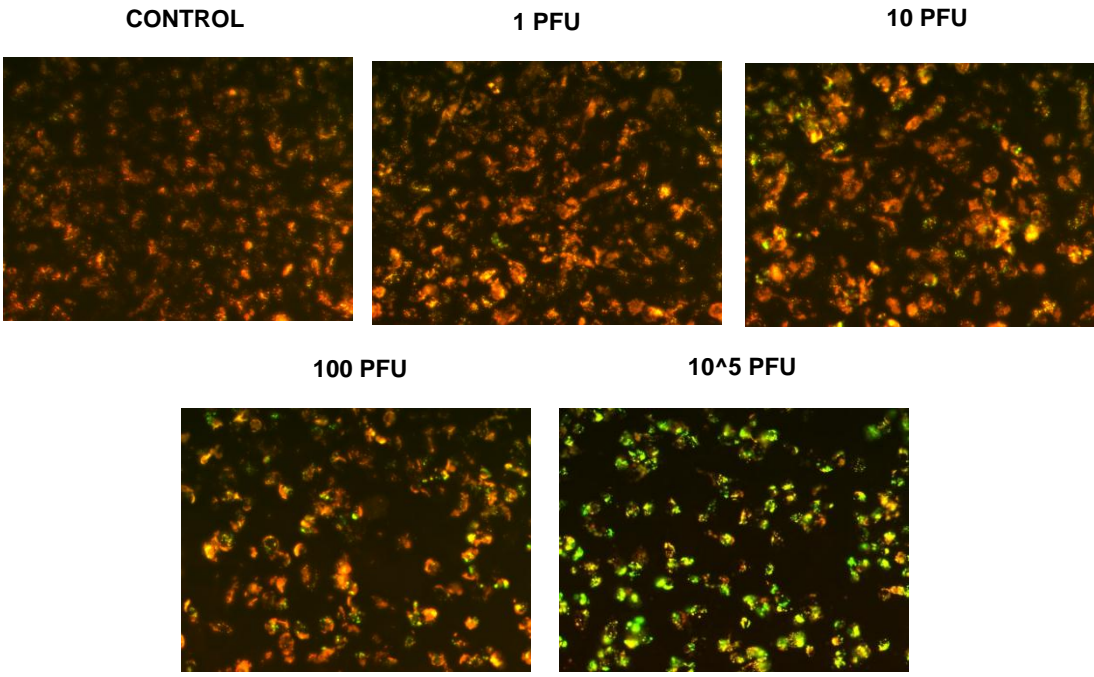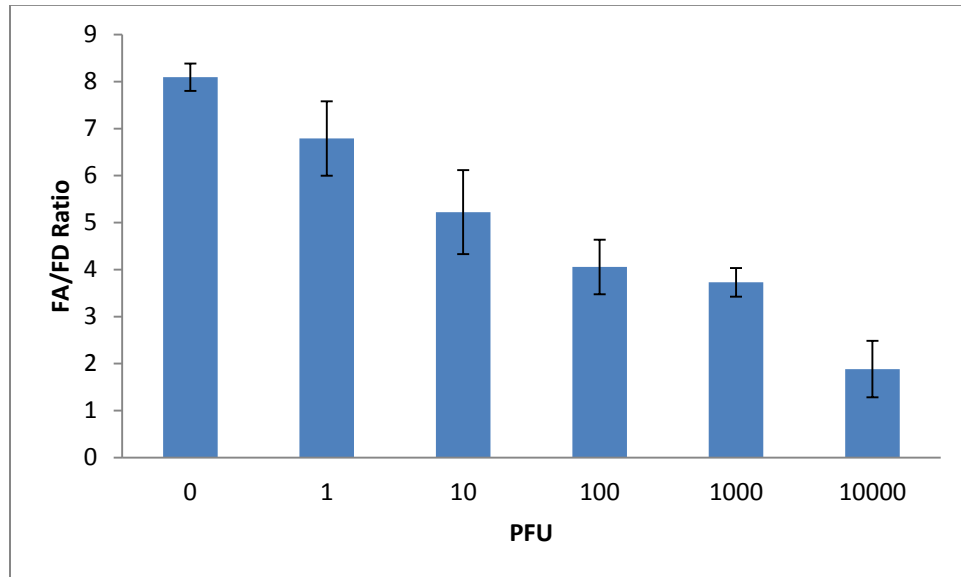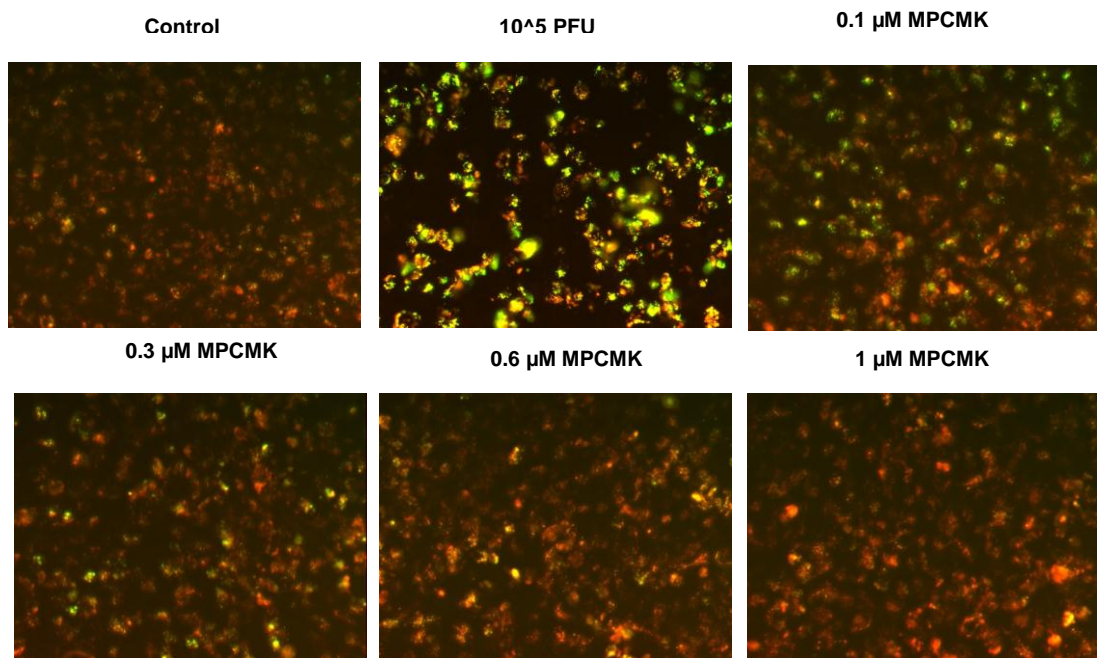**Fig. 4.1.**

Fig. 4.2.

Fig. 4.3.

Fig. 4.4.

QD FILTER EX 435/EM 535   FRET FILTER EX 435/EM 610   MERGED IMAGE

DIC IMAGE   MERGED COMPOSITE

Fig. 4.5.

CONTROL   1 PFU   10 PFU

100 PFU   10^5 PFU

Fig. 4.6.

Fig. 4.7.

Control	10^5 PFU	0.1 µM MPCMK

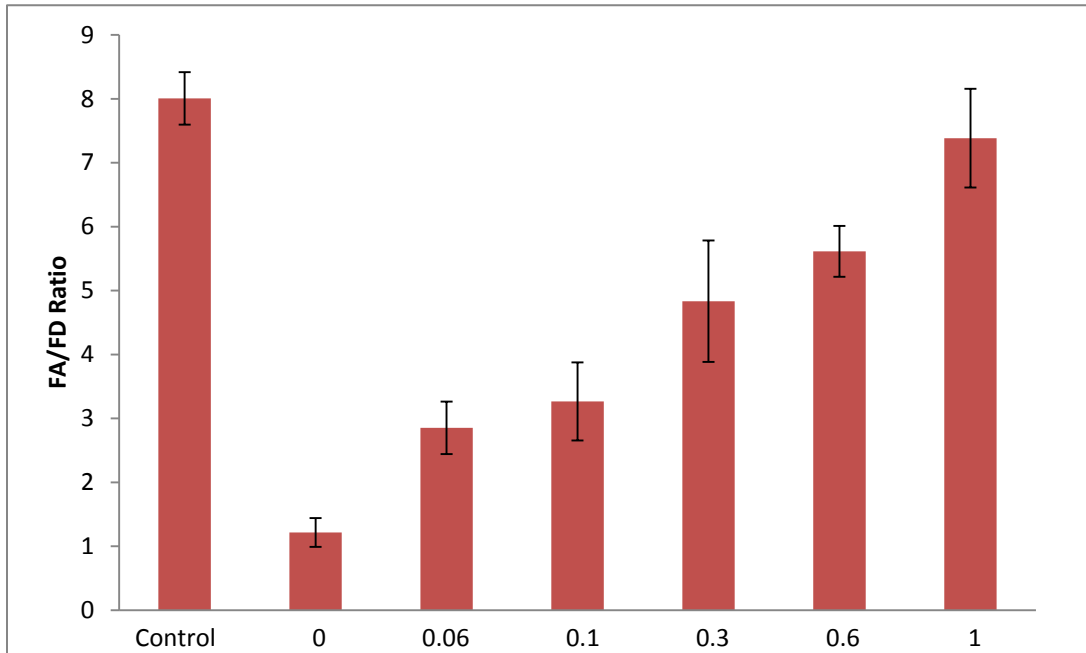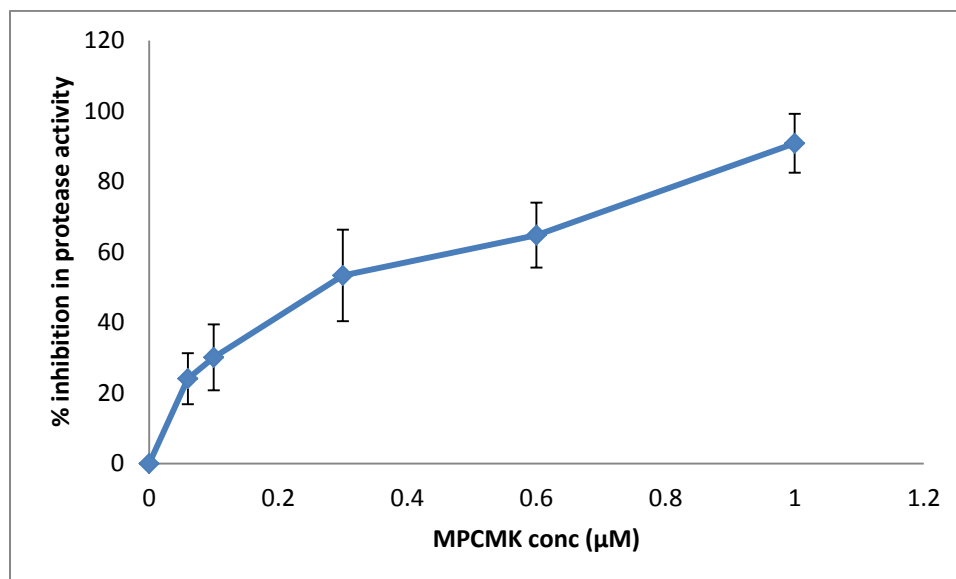| 0.3 µM MPCMK	0.6 µM MPCMK	1 µM MPCMK

Fig. 4.8.

Fig. 4.9.

Conclusion

Viruses pose a threat to public health and safety due to their ease of transmission with high morbidity rates at low infectious doses. To prevent the spread of disease and provide timely clinical management, a simple, rapid and efficient detection method is necessary. In this thesis fluorescent probes were designed to detect the presence of infectious viruses in living cells and provide a better understanding of the disease progression process. The use of fluorescence probes in conjunction with fluorescence microscopy allowed us to study the time course of viral infection and obtain vital information that will be useful for drug development. We developed several FRET (fluorescence resonance energy transfer)-based MBs to directly visualize the fluorescent hybrids with viral RNA as an indication of viral infection. The combination of nuclease-resistant constituents and Tat peptide delivery resulted in an improved efficiency of the beacon, i.e., real-time monitoring of viral infection. MBs were designed to characterize the poliovirus infection in BGMK cells. While fluorescence microscopy was used to visualize the dynamics of viral infection, flow cytometry (FC) based assay offered an automated platform to provide quantitative information to systematically monitor and characterize the propagation of the virus in mammalian cells. Using a combined MB-FC based method, high-throughput detection of PV1 infected cells was achieved with minimal cell pre-treatment. This MB flow based detection scheme is simple, robust and offers several advantages to be adapted into a diagnostic test in viral laboratories. The high sensitivity (less that 1% infected cells) of the assay combined with the rapid detection of infected cells (less than 15 min) make it an exceptional candidate to detect epidemiologically more important viruses. The high degree of specificity of the beacons

was exploited to perform comparative studies with different subtypes of influenza A virus. The specific nature of these probes can be used to perform co-infection studies and subtyping of influenza A virus. Ultimately, we hope that this technique will be tailored into a rapid diagnostic test based format for the accurate identification of influenza virus.

Another approach to detect the presence of infectious viruses was explored by probing the viral protease activity *in vivo.* A genetically engineered protein module was designed using quantum dot (QD) based FRET substrates to work as nanosensors for sensing protease activity. The in house production of peptides caused a significant reduction on the cost of peptide synthesis. Also, this method enabled rapid production and purification of the peptides. Another important feature of these nanosensors was the TAT peptide based delivery method to efficiently deliver the probes across the cell membrane. The effectiveness of the FRET substrate to detect intracellular viral protease activity in a rapid, sensitive manner was demonstrated. More importantly, this QD-FRET based cell assay system could be used to monitor protease activity in response to inhibitors. Therefore this technique can be an ideal platform for high-throughput screening of inhibitors of viral protease.